U. S. DEPARTMENT OF THE INTERIOR

U. S. GEOLOGICAL SURVEY

Geothermal Resources in the Crater Lake Area, Oregon

by

Charles R. Bacon[1]

and

Manuel Nathenson[1]

OPEN-FILE REPORT 96-663

[1]Mail Stop 910, 345 Middlefield Road, Menlo Park, California 94025-3591

1996

11/1/96

Contents

Geothermal Resources in the Crater Lake Area, Oregon

by

Charles R. Bacon and Manuel Nathenson

Summary

The main source of heat in the upper crust in the Crater Lake area is the magma chamber that was responsible for the caldera-forming eruption 7,700 years ago. The amount of heat transferred to the upper crust during development of the chamber and the heat stored in the remains of the chamber following eruption have been estimated on the basis of geologic data and petrologic models. Some of this heat currently is being lost through discharge of the springs of the Wood River group and through venting of fluids to Crater Lake, manifestations of the *Crater Lake hydrothermal system.* Accounting for all of the heat sources and losses results in a minimum total heat content of the upper crust today of 375×10^{18} joules. The separate *Mazama hydrothermal system* is identified on the basis of data obtained from a drill hole immediately east of Crater Lake National Park, MZI-11A. This system may be supplied by intrusions related to Pleistocene volcanic rocks near the east rim of the caldera.

Introduction

Crater Lake caldera serves as spectacular evidence for the recent existence of a shallow magma body in the Cascades. Given the recency of the eruption responsible for collapse of the caldera and the long history of volcanism there (see below), it is logical that one or more geothermal systems should exist in or adjacent to Crater Lake National Park. Because of this, the U.S. Geological Survey undertook detailed studies of the eruptive history of Mount Mazama, the characteristics of the volcanic rocks, and the chemistry of surface waters.

Modern geological maps of Crater Lake National Park and its surroundings are the 1:250,000 scale maps of the Medford quadrangle (Smith, and others, 1982) and the west halves of the Klamath Falls (Sherrod and Pickthorn, 1992) and Crescent (MacLeod and Sherrod, 1992) quadrangles, Sherrod's (1991) 1:125,000 map of the area north of Crater Lake, and Bacon's (unpublished, 1995) 1:24,000 scale map of Mount Mazama. Geological data used in this paper are primarily from the last source and from supporting publications and unpublished data (including K–Ar dates by M. A. Lanphere), as they cover the area of potential geothermal reservoirs associated with Mount Mazama. Information also is included from preliminary examination of core obtained from two exploration wells drilled by California Energy Company. There are no published geophysical studies of sufficient detail to be useful in evaluating geothermal resources of the area. However, geoelectrical surveys were conducted outside Crater Lake National Park by Harve Waff (University of Oregon) for California Energy Company.

Much has been learned about the hydrothermal system(s) of Mount Mazama since the last USGS assessment of geothermal resources in the Cascades (Brook and others, 1979). Crater Lake has been the subject of intense study because of the question of whether or not there is a significant thermal feature in the lake (Collier and others, 1991), and temperature measurements are available from the two wells drilled by California Energy Company (Blackwell, 1994). These data are discussed in the second part of this report.

Geological Considerations

Mount Mazama and Crater Lake caldera lie at the intersection of the High Cascade chain of volcanoes with the Klamath graben, a north-northwest-trending basin bounded by faults whose displacement is mainly in a vertical sense (Figure 1). At this latitude, the western margin of the Basin and Range province, characterized by north–south- to northwest–southeast-trending faults, impinges upon the High Cascades. Focusing of volcanism at Crater Lake and the longevity of this complex volcanic center are undoubtedly linked to the regional tectonic situation. North and south of Crater Lake there are many shield volcanoes of modest size and many more cinder cones with associated lava flow fields. The latter represent short-lived activity at isolated vents (monogenetic volcanoes). The shields and monogenetic volcanoes are a manifestation of the regional flux of magma all along the Cascades.

Underneath Mount Mazama

Beneath the east half of Mount Mazama is a 16x24 km field of older rhyodacite lava (≥400 ka; probably ~20 km^3 of rock; Nakada and others, 1994), itself resting on basaltic andesite on its southwest side and on andesite and dacite on the southeast (Figure 2). Core from the 1423-m-deep MZI-11A drill hole 6 km east-southeast of the caldera (Figure 3) indicates that the rhyodacite is underlain beginning at a depth of 229 m by 472 m of hornblende-bearing andesite or dacite (probably the flank of a composite volcano), 422 m of mafic lava flows perhaps equivalent to those exposed on the east of the Klamath graben, and >300 m of silicic tuffs that dip significantly and may be correlative with rocks in the Western Cascades. Twelve km south of the caldera, the 867-m-deep MZII-1 drill hole encountered basaltic or basaltic andesitic lavas and minor tuffs beneath 64 m of unconsolidated deposits (probably reworked ejecta from the caldera-forming eruption); below 342 m in the lava section is a 414-m-thick basalt and basaltic andesite sill(?).

Structural setting

Faults defining the east and west sides of the Klamath graben continue north toward Mount Mazama (East Klamath Lake and West Klamath Lake fault zones on Figure 1). The West Klamath Lake fault zone passes just west of Crater Lake caldera, where it is represented by the north-south-trending, down-to-the-east Annie Spring and Red Cone Spring normal faults (Figure 2). The Annie Spring fault cuts Mazama lavas as young as ~50 ka on the southwest of the volcano <1 km from the caldera. The Red Cone Spring fault cuts basaltic andesite of Red Cone dated at ~35 ka. Offset lava flows dated by the K-Ar method suggest a long-term average slip rate of 0.3 mm/yr for the Annie Spring and Red Cone Spring faults for the last ~300,000 years. This result is consistent with measurements of offsets in glacial moraines at the mouths of Threemile, Sevenmile, and Cherry Creeks further south along the West Klamath Lake fault zone (Hawkins and others, 1989). The West Klamath Lake fault zone is believed to be capable of a magnitude 6 to 7 earthquake (Bacon and others, in preparation).

Other north-south normal faults cut older rocks between the West Klamath Lake fault zone and approximately the west boundary of Crater Lake National Park (Figure 1). Normal faults that trend toward Mount Mazama from the East Klamath lake fault zone are buried by 400-200 ka lavas. North-northeast-trending, down-to-the east normal faults are buried by deposits of the climactic eruption and ≥400 ka pre-Mazama rhyodacite lava flows east of Mount Mazama. North-south vent alignments are evident southwest and northwest of Mount Mazama, and similarly oriented dikes are exposed in the glaciated terrain in the southwest quadrant of the park. Vent alignments, dikes, and faults all indicate ~east-west extension. The area is undergoing slow extension and has been for a long time because older rocks are offset more than younger ones. This regional fault system influences groundwater flow, as is clear from the occurrence of springs along the East Klamath Lake fault zone that feed the Wood River and other nearby streams and along the West Klamath Lake fault zone.

Seismicity of Crater Lake and vicinity

There is a significant variation in rates of seismicity along the Cascade Range, with the area south of Mount Hood in Oregon being particularly quiet compared to other parts of the Cascades (Weaver, 1989). A four station array along with an ultraportable outlier station operated in the summer of 1970 at Crater Lake found that there were fewer small events at Crater Lake than at Mount Hood (Westhusing, 1973). No events were deeper than 12 km. There is, however, a sparse record of seismicity at Crater Lake and its vicinity (Table 2 and Figure 4). The largest event took place in 1920 before there were almost any seismometers in Oregon, is known to have been felt at Intensity V, and has an estimated magnitude of 4+ (see references to Table 2 for sources of data). The location of the event is quite uncertain, though it is thought to have been near Crater Lake. In 1947 there was an event with estimated magnitude of 3.7 south of Crater Lake near the town of Fort Klamath. One felt event in 1982 occurred near Crater Lake while a temporary array was deployed in Oregon (Kollmann and Zollweg, 1984). A relocation of this event by R. S. Ludwin (written communication, 1996) has moved the event closer to Crater Lake and reduced its magnitude to 1.7 from the 2.5 calculated by Kollmann and Zollweg (1984). Subsequent to the Klamath Falls earthquakes of 1993 (located south of the map area in Figure 4), telemetered instruments were added to monitor the seismicity after those earthquakes (University of Washington, 1993), and locations and detection limits for earthquakes in the vicinity of Crater Lake improved. The event shown on the map for 1993 took place a few hours after the second Klamath Falls earthquake (a magnitude 6.0) and still has a considerable uncertainty of location. The map of earthquakes in Washington and Oregon from 1872-1993 (Goter, 1994) shows a scattering of seismicity stretching northward from Klamath Falls to Crater Lake. The catalogue for these earthquakes (R. S. Ludwin, written communication, 1996) shows that they are preliminary locations of aftershocks from the 1993 Klamath Falls earthquakes as located by the Northern California Seismic Network. Subsequent work has shown that the aftershocks do not go as far north as shown on Goter's map (Qamar and Meagher, 1993).

In 1994 and 1995, there was a significant amount of seismicity associated with Crater Lake. The event of 94/1/26 west of Crater Lake is noteworthy in having a depth of 42 km and low-frequency wave form. In May, there were two events in the vicinity of the 1947 events near Fort Klamath. In December, there were three events (two felt) just south of Crater Lake. The depths for the two well-located events are quite shallow, indicating that they are probably tectonic rather than magmatic. In August of 1995, there were three more events near Fort Klamath.

Fault planes exposed by quarrying in the Klamath Basin have steep dips (~60°) and appear to record mainly vertical displacement. Earthquake epicenters shown in Figure 4 may be associated with slip at depth on specific mapped faults, given the direction of dip of the faults, focal depths of earthquakes, and imprecision of earthquake locations. The earthquakes south of Crater Lake National Park and west of latitude 122° may have occurred along bounding faults of the Klamath graben. The 93/09/21 event may have been on the Sky Lakes fault zone, but uncertainties could place it further south as part of the Klamath Falls aftershock sequence.

Because of the improved instrumentation, the series of events in 1994 and 95 may be partly a result of better detection. Also, there is some chance that some of these events could be in response to the Klamath Falls earthquakes of 1993. Many of the events are within the Klamath graben structure, which extends from south of Crater Lake to beyond Klamath Falls. Because of burial by Mount Mazama itself, the northerly limit of this structure is unknown. Note, however, that faults contiguous with the West Klamath Lake fault zone pass just west of Crater Lake caldera and continue on to the north (Figures 1 and 2). The area around Klamath Falls in the Klamath graben has had significantly more seismicity in the last 50 years than has Crater Lake (see list in Sherrod, 1993). Earthquakes documented in Table 2 are not very abundant considering the probable size and state of the Crater Lake magma chamber, the number of tectonic faults in the region, fault scarp heights, and the known recency of displacement on the West Klamath Lake fault zone. Given the short recorded history of human occupation of the Crater Lake area, this could be an anomalously quiet time.

Monogenetic volcanoes

Besides Mount Mazama, other volcanoes in the park are monogenetic shields and cinder cones that erupted basalt, basaltic andesite, and andesite from before the onset of Mazama volcanism until as recently as early Holocene time (Bacon, 1990; Bacon and others, 1994). High-alumina olivine tholeiitic basalts (HAOT) occur along the Rogue River south of latitude ~42°56' (apparently ~1 Ma in age there), erupted from a vent 2 km east-southeast of Bald Crater, and can be traced in Castle Creek to within 8 km of the caldera, where they are buried by climactic ignimbrite. Early Holocene HAOT, the youngest mafic lava in the area, vented at three places near Castle Point. Other tholeiitic basalts northwest of the caldera may be late Pleistocene. Similar rocks are present elsewhere in and east of the Cascades (Hart and others, 1984). They represent melts from depleted mantle that has been modestly enriched in large-ion lithophile elements (LILE) (Bacon and others, 1994). Most HAOT in the Crater Lake area did not experience large amounts of differentiation in the crust and, therefore, are of little geothermal significance other than to indicate the longevity and areal extent of mantle-derived magmatism.

Vents that produced LILE-rich calc-alkaline basalt, basaltic andesite, and andesite are far more numerous than those that erupted HAOT. The least differentiated of the calc-alkaline magmas originated in mantle domains that are notably enriched in LILE as a result of modern subduction of the Juan de Fuca and Gorda plates (Bacon and others, 1994). The calc-alkaline lavas of monogenetic vents are similar to magmas that fed the Mazama magmatic system.

Vents for *crystal-rich* calc-alkaline basaltic andesite and andesite occur only within ~6 km of the caldera and are ≤100 ka in age. This observation has significance for geothermal resource potential. The crystals provide evidence for subsurface cooling of magma, as most of the crystals in these lavas appear to be derived from cumulate crystal mush or gabbro, presumably resident in the mid to upper(?) crust because of focusing of intrusion near Mount Mazama. Crystallization, partial or complete, requires loss of significant amounts of heat to wallrocks and therefore may provide a heat source for geothermal systems.

Vents for basaltic andesite and andesite surround Mount Mazama (Figure 1), although ages vary widely and there generally are few vents in any given area. High Cascades basaltic andesites are exposed as far west of Mount Mazama as the Rogue River (longitude ~122°27'), which approximately marks the boundary with the Western Cascades (~122°30'), but there is only one known <100 ka vent west of Mount Mazama (other than early Holocene HAOT near Castle Point; compare Figure 1 with Figure 2). Similarly, east of the caldera there is only one lava flow (andesite of Scott Creek) from a monogenetic vent that is <100 ka (Figure 1). Most of the monogenetic eruptive activity occurred north and south of Mount Mazama, along an 10-15-km-wide zone that might be called the High Cascades axis. Magma feeding the Mazama magmatic system beneath the main edifice presumably would have been intruded dominantly along this same zone. Within 8 km of the caldera rim there are 8 known vent areas that are ≤100 ka in age. There are indications that most of the younger basaltic andesitic and andesitic magmas were rich in H_2O, such as the ~40 ka lavas of Red Cone (c. 1-2 km^3) and the large (>8 km^3), ~20 (?) ka Timber Crater shield. This property may have aided in development of the high-level chamber containing fractionated silicic magma.

Mount Mazama proper

Mount Mazama was made up of several overlapping basaltic andesitic to dacitic shield and stratovolcanoes, including flank vents that produced thick lava flows, active episodically from ≥400 ka to ~40 ka (Bacon and Lanphere, 1990). The center of active volcanism gradually migrated west-northwestward as the volcano grew. Rocks older than ~100 ka commonly are hydrothermally altered in caldera wall exposures. Glacial ice was present high on Mount Mazama throughout much of its history and descended as valley glaciers several times.

The composite volcano of Mount Mazama (Figure 2) initially erupted low-silica dacite with abundant andesitic enclaves (inclusions of chilled magma drawn up from deeper in the system) c. 400 ka. In the ensuing 300,000 years, many sequences of low-silica dacite, andesite, and, locally, basaltic andesite lavas vented from different centers, each for a comparatively brief period, to build the edifice. The duration and the temporal continuity of volcanism near Crater Lake are similar to those of other Cascade volcanic centers (e.g., Lassen: Clynne, 1990; Mount Adams: Hildreth and Lanphere, 1994).

At about 70 ka, several km^3 of dacite erupted as lava flows and pumice falls (tephra of Pumice Castle). During the same period, hornblende basaltic andesite and pyroxene andesite, both rich in LILE and H_2O, built a large composite cone (part of Mount Mazama) that includes what is now Hillman Peak on the west rim of the caldera. Vents for the dacitic eruptions spanned a WNW-ESE distance of 7 km, so there may have been a sizable, integrated magma body at that time. The most voluminous of these dacitic lavas and pyroclastic rocks that remain after collapse of Crater Lake caldera vented on the east near Cloudcap. The intensity of volcanic activity at ~70 ka, and particularly the eruption of voluminous dacite, suggest that related intrusions may still exist as significant heat sources.

Andesite again erupted and formed lava flows on the southwest and north slopes of the volcano around 45-50 ka. Dacitic eruptions occurred at ~50 ka, producing a pyroclastic flow and The Watchman lava flow, and again ~35 ka, when dome(s) were emplaced southwest of Mazama's summit and Williams Crater was active (basaltic andesite mingled with dacite; Figure 2). After this time, only rhyodacite erupted until near the end of the climactic eruption.

The last 30,000 years

Crater Lake partly fills the 8x10 km diameter caldera that collapsed ~7700 years ago (6845±50 yr. B.P. ^{14}C date: Bacon, 1983) during the climactic eruption of Mount Mazama. This eruption vented ~50 km^3 of mainly rhyodacitic magma. After the andesitic and dacitic eruptions of Mount Mazama had ceased, the shallow magma chamber responsible for the catastrophic eruption produced several rhyodacite lava flows and associated pumice deposits between ~30 and 24 ka, and in the last few hundred years before the climactic eruption (Bacon and Druitt, 1988). This chamber lay at a depth of ≥5 km (Bacon and others, 1992) and developed in the remains of an older granodiorite pluton (Bacon and others, 1989; Bacon, 1992). The climactic eruption took place over a few days, toward the end of which the caldera collapsed. This eruption produced a classic, compositionally zoned pyroclastic deposit that represents the rather orderly venting of a shallow, stratified magma body (Druitt and Bacon, 1986, 1988, 1989; Bacon and Druitt, 1988). Pumiceous pyroclastic-flow deposits fill valleys around Mount Mazama to depths of ~100 m (Figure 2) and extend as much as 70 km from the caldera. Unconsolidated lithic breccia, which is the proximal facies of the pyroclastic flows, occupies the heads of valleys and is found on the slopes of Mount Mazama. These two units drastically affect surface drainage and shallow groundwater flow.

Postcaldera volcanic activity was restricted to the caldera (Figure 5). Andesitic lava and pyroclastic material formed the central platform, Merriam Cone, and Wizard Island within a few hundred years of caldera collapse, while the lake was filling. A small rhyodacite dome east of Wizard Island was emplaced later, ~5000 yr. B.P. (~4000 ^{14}C yr. B.P.)

Products of the climactic magma chamber

The shallow body of magma which fed the caldera-forming eruption of Mount Mazama is known as the climactic magma chamber (Bacon, 1983). The growth and compositional evolution of its magmas can be tracked through study of rhyodacite lava domes and their enclaves leaked from the chamber from ~30 ka until the time of the climactic eruption (Bacon and Druitt, 1988).

The first erupted products of the climactic magma chamber are believed to be the differentiated rhyodacite that forms the ~30-24 ka flows of Grouse Hill, Steel Bay, and Redcloud Cliff (Bacon and Druitt, 1988; Figure 2). These contain andesitic enclaves with moderate LILE contents (enclaves in Holocene rhyodacites have notably higher LILE concentrations), are hornblende phryic, and have lower phenocryst equilibration temperatures (850°C versus mainly 880°C) than younger rhyodacites (Druitt and Bacon, 1989).

The first known eruptions of rhyodacite compositionally identical to the climactic ejecta resulted in emplacement of the 12 small domes of the Sharp Peak group on a radial trend northeast of the caldera. Textures of these rocks and lack of any known correlative tephra suggest they vented degassed magma from a dike, probably moving laterally from the climactic chamber. The age of the Sharp Peak domes is uncertain. They have been slightly modified by glaciation at an elevation of 5500-6000 ft, suggesting they are >13 ka, and their paleomagnetic pole position suggests an age between Redcloud Cliff and Holocene rhyodacites (Bacon and Druitt, 1988). Their pre-eruptive temperature was identical to that of the climactic rhyodacite (see below). A small, late Pleistocene rhyodacite dome south of Crater Lake at Bear Bluff also may have been fed by a lateral dike from the climactic magma chamber.

Holocene eruptions from the climactic chamber first produced the Llao Rock pumice fall and lava flow (7015±45 ^{14}C yr. B.P. = 7890±74 calendar yr. before 1990; conversion to calendar years through tree-ring calibration), then the Cleetwood pumice fall and lava flow. Because the Cleetwood flow was still hot when the climactic eruption started (Bacon, 1983), the ages of Cleetwood and climactic events are the same within the resolution of any of our dating methods (climactic eruption: 6845±50 ^{14}C yr. B.P. = 7708±62 calendar yr. before 1990). The Llao Rock magma was somewhat more differentiated than, and the Cleetwood identical to, the climactic rhyodacite. Preeruptive temperatures ranged from about 850°C for early Llao Rock pumice to 880°C for late Llao Rock and the other rhyodacites (Druitt and Bacon, 1989). The Llao Rock eruption tapped a local pocket of differentiated magma near the roof or margin of the chamber. Compositional and thermal uniformity of climactic rhyodacite indicates that the main volume of silicic magma was vigorously convecting. The Cleetwood and Llao Rock lavas contain andesitic enclaves with LILE contents that are different for the two units and greater than those of inclusions in the 24-30 ka rhyodacites. Presence of enclaves with different trace element abundances indicates that the climactic chamber was fed by several discrete pulses of andesitic magma.

Bacon and Druitt (1988) considered the enclaves in the rhyodacites to be samples of "new" parent magma from which younger rhyodacite magma evolved. A model for this process is given in Bacon and Druitt (1988) and Druitt and Bacon (1988, 1989). Figures 6 and 7 depict the magma chamber and the properties of its contents. The climactic rhyodacite was underlain by cumulate mush whose temperature increased downward. The chamber apparently grew incrementally over a period of >23,000 yr by injection of mostly andesitic magma. If the minimum area of the chamber can be represented by the subsided part of the caldera floor, it represents a disk about 5 km in diameter. As 50 km^3 of magma erupted, mostly rhyodacite but including subordinate andesitic to basaltic crystal mush, the chamber could have been 2-3 km thick. Reasonable additions of appropriate volumes of cumulates (Druitt and Bacon, 1989) and increases in the diameter of the chamber offset each other, so that the thickness of material known to have been above solidus temperature probably was between 2 and perhaps 5 km. The depth to the top of the chamber was ≥5 km (Bacon, and others, 1992).

Granitic rocks

Granodiorite and related rocks ejected as blocks during the climactic eruption show that the deep walls of the chamber were melting at the time of the eruption (Bacon and others, 1989; Bacon, 1992). These granitic rocks were quarried by the eruptive process from an unexposed high-level pluton very like the Tatoosh pluton near Mount Rainier (Fiske and others, 1963). Strontium isotope systematics imply that the pluton is Miocene in age (Bacon and others, 1994). The pluton underlies at least the ~20 km^2 area within the structural boundaries of the caldera.

Oxygen isotope data indicate that the granitic rocks exchanged with low-^{18}O meteoric hydrothermal fluids to varying degrees before reequilibrating at high temperature (Bacon and others, 1989), which reached 1000°C in some samples (Bacon, 1992). New analyses of quartz and plagioclase in unmelted granodiorite from the climactic ejecta and from two samples from Pleistocene eruptive units suggest that the hydrothermal alteration commenced between ~70 (dacite of Pumice Castle) and 24 ka (rhyodacite of Redcloud Cliff; Bacon, 1992). Hydrothermal exchange is facilitated in areas of extensional tectonics, such as the vicinity of Crater Lake and the Klamath graben. The above data and observations on the granitic rocks suggest that: (1) one or more hydrothermal systems were active over an area of ≥20 km^2 (area of subsided block of caldera; granitic blocks occur in the ejecta all around the caldera) as the climactic magma chamber was developing; (2) the immediate wall rocks to the chamber became closed to fluid flow as local temperature increased during growth of the chamber; (3) heat from the magma chamber was moving through the immediate walls by conduction (the width of the conductive zone is unknown and could have been rather small).

Postcaldera volcanism

The spectacular compositional zonation of the climactic ejecta and the dominance of dense, crystal-rich blocks at the top of the section suggest that much of the silicic magma in the chamber erupted in the caldera-forming event. However, physical models of zoned eruptions suggest that this is unlikely. Postcaldera volcanism gives a clue but does not entirely resolve the issue. About 3 km^3 of andesite was erupted in a period of a few hundred years after caldera collapse (Nelson and others, 1994) from vents in the central, western, and northern regions of the caldera (Figure 5). This andesite may be a hybrid of left-over rhyodacite and crystal mush, or, more likely, may be "new" magma. A small hornblende rhyodacite dome (c. 0.03 km^3) was emplaced on the east flank of Wizard Island about 5000 yr. B.P.. The preeruptive temperature of this rhyodacite was 840°C. It probably is a differentiate of postcaldera andesitic magma (now largely crystallized), but its composition has not been reproduced by any simple model. The character of postcaldera volcanism suggests that Crater Lake remains a focus of magmatic activity but that a large, shallow body of crystal-poor silicic magma probably is no longer present. Magma remaining in the chamber after the climactic eruption may have crystallized to the point where it is too viscous to erupt.

Nature of the crustal magmatic heat source

The observations enumerated above indicate that magmas have been crystallizing in the mid- to upper crust beneath Mount Mazama off and on for >400,000 yr. The most recent documented episode, in which the climactic magma chamber developed, affected an area of 20 km^2 and possibly 75 km^2 (a somewhat arbitrary maximum value). The upper surface of that magma body lay at ≥5 km depth and was at 880°C 7700 yr. ago. Near its geographic center, it was still at 840°C 5000 yr. ago (pre-eruptive temperature of postcaldera rhyodacite). We have no information on its present thermal state.

Estimate of magmatic heat

A *minimum* estimate of heat transferred from the climactic magma chamber to its surroundings can be obtained from the volume of crystal cumulates estimated by Druitt and Bacon (1989, p. 258). If we assume the ~50 km^3 of magma ejected in the climactic eruption represents *all* of the contiguous silicic magma that was present 7700 yr. ago, a limiting case which will result in a minimum heat value, and that as a first approximation all of that magma formed by differentiation of andesitic magma, then ~150 km^3 of cumulates should have been produced. Formation of the cumulates would have involved cooling of hydrous andesitic magma from a 1030 °C near-liquidus temperature to the 880°C preeruptive temperature of the rhyodacite and growth of crystals while the residual liquid evolved to silicic composition. The heat liberated by this process would consist of contributions from three sources: (1) latent heat of crystallization of ~100 km^3 of crystals (the cumulates are approximately two-thirds crystallized); (2) heat content of the crystals and the liquid from which they grew; and (3) heat content of the ~100 km^3 of silicate liquid (~50 km^3 ejected plus ~50 km^3 remaining as intergranular residual liquid in the cumulate mush). An estimate of the total heat liberated can be obtained in the following manner. The ~100 km^3 of hydrous rhyodacite and residual melt had a mass of 2.2×10^{17} g and the crystals a mass of 2.9×10^{17} g (for densities of 2.2 and 2.9 g cm^{-3}, respectively). We approximate the modal compositon of the cumulate crystals by a 3:1 plagioclase:mafics mixture and calculate a latent heat of crystallization of 446 joule g^{-1} (estimated from heats of fusion given by Lange and Carmichael, 1990), or 129×10^{18} joule for the assumed mass of crystals. The specific heat of this mixture of crystals is a nearly linear function of temperature over the interval 880-1030°C and can be approximated as 1.22 joule g^{-1} deg^{-1} (Robie and others, 1978). The specific heats of silicate liquids, which are approximately temperature-independent, can be calculated from the liquid compositions using the partial molar heat capacities given by Stebbins and other (1984), yielding values of 1.39 joule g^{-1} deg^{-1} and 1.43 joule g^{-1} deg^{-1} for rhyodacite and andesite, respectively. Because of the temperature invarience of the specific heats in question, we approximate the specific heat of crystallizing andesitic magma as the mean of the values for the crystal mixture and rhyodacitic melt, *i.e.*, 1.31 joule g^{-1} deg^{-1}. Multiplying by the mass and temperature change gives 57×10^{18} joule for (2). Component (3) is simply the mass of rhyodacite times its specific heat times the temperature change, or 43×10^{18} joule. Summing all three contributions gives a rounded (minimum) value of 230×10^{18} joule for the total heat liberated during differentiation of the climactic magma chamber (Table 1).

The differentiation process appears to have taken place over a period of ~30,000 years, and the average rate of heat loss to form the crystals would be 240 MW_t. On the other hand, using the formula in Smith and Shaw (1975, p. 62), the total heat transfer for a conductive model of a 20 km^2 magma chamber would be 42×10^{18} joules. Thus the total heat transfer resulting from cooling and crystal growth is over five times what one would estimate based on a conductive model (Table 1). The conductive model has most of the heat transfer taking place early in the time period because the heat transfer rate decreases with the square root of time. We believe that the crystallization model is superior to the conductive one because it is based on data specific to the Mazama magma chamber.

The minimum total heat remaining in the chamber at the end of the climactic eruption can be estimated at 400×10^{18} joule (Table 1) by calculating the heat that would be liberated by crystallization of the above-hypothesized 50 km^3 of intergranular liquid (~50×10^{18} joule) and the change in enthalpy of the resulting crystals, plus 100 km^3 of cumulus crystals (total of 4.0×10^{17} g), in cooling to 25°C (H_{880}-$H_{25} \approx 875$ joule g^{-1} of crystals; estimated from heat contents given by Robie and others, 1978). The minimum total heat added to the upper crust is then 230+400 = 630×10^{18} joules. A more sophisticated thermal model is not warranted because of significant uncertainty in the volume of the system. Assuming that the current rate of hydrothermal convective heat loss of 102 MW_t (see *Surface thermal data*) has persisted for 7700 years (Table 1), which is probably a minimum estimate of convective heat loss, the chamber and the surrounding upper crustal rocks would have lost 25×10^{18} joules (at this rate, the heat currently in the chamber would be dissipated in ~90,000 yr.). In comparison, the conductive formula in Smith and Shaw for a 20 km^2 chamber yields a conductive heat loss estimate of 21×10^{18} joules.

The total heat currently in the upper crust probably is less than our estimate of ~630×10^{18} joules for the heat added to the upper crust. The heat lost from the chamber during crystallization (230×10^{18} joules) may have been added to thermal water and then discharged to the surface. At the current rate of hydrothermal convective heat loss, the convective heat flow over the last 7700 years has probably removed at least 25×10^{18} joules from the chamber. If the rate of convective heat transfer has been decreasing since the climactic eruption, as suggested by silica spires on the lake floor (Figure 8; see *Water geochemistry*), additional heat may have been lost from the chamber. If we assume that both the heat lost during differentiation of the climactic magma (230×10^{18} joules) and the hydrothermal heat flux subsequent to the climactic eruption (25×10^{18} joules) were removed from the upper crust, the chamber still has ~375×10^{18} joules of stored thermal energy (Table 1), which is still quite a large upper-crustal thermal anomaly. In comparison, Smith and Shaw (1975) estimated that the heat stored currently in the magma chamber is 770×10^{18} joules by assuming a chamber volume of 320 km^3 and that the most recent eruption was 700 years ago. Although the stored heat estimates are quite comparable (somewhat fortuitously), we believe that our estimate of 375×10^{18} joules (Table 1) is more realistic than that of Smith and Shaw because it takes hydrothermal convection into consideration and is based on new information on volumes, ages, and magma chamber dynamics. We believe that the most appropriate value for the time since the last eruption is 7700 years because all postcaldera andesitic volcanism ceased within a few hundred years of that time and because the 5000-year-old rhyodacite dome appears to represent a volumetrically insignificant eruption of liquid related to cooling of the remains of the magma chamber.

If we accept the minimum chamber area of 20 km^2 and assume that the roof of the climactic magma chamber was at 5 km, eruption of 50 km^3 of magma would have lowered the roof by 2.5 km to a depth of 7.5 km. The remaining thermal energy in the hypothesized cylindrical magma chamber would then lie between the depths of 7.5 and 15 km. In all likelihood, however, the chamber was not strictly cylindrical and was larger than the 20 km^2 minimum area, so that the subsidence of the roof indicated by Crater Lake caldera would have preserved an annular shallow heat reservoir. All of the caveats in Smith and Shaw (1975) apply to the present estimate of heat in the upper crust (e.g., preheating, continuing addition of andesitic or basaltic magma, hydrothermal circulative loss, etc.).

Modification of the stored heat estimate most likely would increase it because the magma chamber volume on which it is based is a minimum value and because all of the heat of crystallization may not have been lost by hydrothermal convection. Moreover, the heat stored in the remains of the climactic magma body and the effect of development of the climactic magma chamber are thought to overwhelm any other source of heat input to the upper crust since the climactic eruption (e.g., cooling of a pluton associated with the >400 ka pre-Mazama rhyodacites, crystallization of intermediate-composition magma during growth of Mount Mazama, development of the source chamber(s) for ~70 ka and younger dacites). It is possible, however, that local heat sources related to pre-climactic magmatism remain viable *outside* the area of the caldera, such as a shallow body a few km in diameter that might be associated with the ~70 ka dacites just east of the caldera or a dike system related to Sharp Peak and associated rhyodacite domes.

Structure of the caldera floor and its relation to hydrothermal systems

Nelson and others (1988) presented results of a seismic reflection study of the caldera floor in which they mapped sediment thickness (up to ~100 m) and identified a ring of possible secondary explosion craters, presumably above a ring fracture zone (Figure 8) marking the boundary of the subsided block and where inflowing groundwater would have encountered hot intracaldera tuff. What lies below "acoustic basement", the maximum depth of recorded seismic reflections, can only be speculated upon. There is probably several hundred m to >1 km of caldera fill consisting of welded tuff and intercalated landslide breccia. This material would rest on the subsided block, or blocks, composed of the remains of Mount Mazama and its underpinnings. Modern hydrothermal systems might form convection cells within the intracaldera section, probably bounded laterally by the ring-fracture zones (considerably inboard of the topographic caldera rim) along which the block(s) subsided. Hydrothermal convection cells outside of the structural limits of the caldera would be expected to be independent of intracaldera cells.

Gravity anomaly of the Crater Lake magma chamber

The characteristics defined above of the probable current state of the Crater Lake magma chamber permit a calculation of what the gravity anomaly should be. The existing magma body is believed to be 150 km^3 in volume with its top at around 7.5 km. Although the shape is likely to approximate a cylinder with an area of 20 km^2 (diameter of 5.0 km) and a thickness of 7.5 km, the gravity signature may be reasonably modeled by a sphere of the same volume with a diameter of 6.6 km. The 2/3 of the volume that is crystals has an assumed density of 2.9 g/cm^3, and the 1/3 that is liquid probably is 2.4 g/cm^3. The average density is thus 2.73 g/cm^3. Williams and others (1988) use a near-surface density of 2.45 g/cm^3 for their Bouguer anomaly map to model the low-densities of volcanic rocks in the upper few kilometers. Williams and Finn (1985) derive a density value of 2.2 g/cm^3 to minimize the anomaly from volcanic topography and to emphasize anomalies from a subvolcanic source in the upper few kilometers. Below a depth of sea level, they assume the surrounding density is 2.45 g/cm^3. At the depth of the Crater Lake magma chamber, densities are likely to be closer to the standard crustal density of 2.67 g/cm^3. Thus the likely density contrast is 2.73 - 2.67 = 0.06 g/cm^3, though the contrast could be as high as 0.3 g/cm^3.

Figure 9 shows the gravity anomaly for a sphere (e.g., Dobrin, 1952, p. 16-17) for two values of density contrast to bracket this range. Gravity anomalies at Crater Lake have been studied by Blank (1968) and Williams and Finn (1985). Williams and Finn (1985) model a subvolcanic intrusion between sea level and -2 km with a density of 2.86 g/cm^3 surrounded by rocks with a density 2.45 g/cm^3 The interpolated gravity anomaly that they model has an amplitude of 15 mgals and represents a volume at depth of more than 25 km^3 of dense material. The anomaly shown in Figure 9 would not be easily separated from the effects of shallower density contrasts modeled by Williams and Finn. The colored gravity map of Williams and others (1988) shows very little radial symmetry that the model for Figure 9 requires, and the anomalies are much larger in amplitude indicating significant density contrasts in the near surface. The Klamath graben, south of Crater Lake, has a pronounced gravity low that can be traced almost to Crater Lake itself. There is clearly a complex three-dimensional density structure in the area of Crater Lake that would make the detection of the anomaly shown in Figure 9 very difficult.

Conclusions from geological information

The vicinity of Mount Mazama and Crater Lake caldera has been a focus of magmatic activity for more than 400,000 years. It is an area of repeated silicic volcanism. The caldera defines the minimum area of a shallow magma chamber that vented some 50 km^3 of magma 7700 years ago. Petrologic information suggests that the depth to this chamber was ~5 km before the caldera collapsed. Crystal cumulates and melt remaining in the climactic chamber, presumably now mainly at depths ≥7.5 km, and the surrounding rocks probably together contain at least 375x10^{18} joules of stored heat.

Hydrothermal system(s) of Mount Mazama

Drill hole and spring data indicate that there are thermal water flows in the caldera and south and east of the caldera on the flanks of the volcano. Data concerning these thermal water flows are presented below, and they permit estimates of stored thermal energy to be made.

Surface thermal data

Figure 1 shows the location of the springs in the Wood River Valley identified as thermal by Nathenson (1990a), and Figure 8 shows thermal springs on the floor of Crater Lake identified by Collier and others (1991). The springs in the Wood River Valley have large flows with temperatures ranging to ~10°C (Nathenson, 1990a). They are thermal springs in the sense of being noticeably higher in temperature than other springs on and around Mount Mazama, but their temperatures are too low to satisfy the definition of thermal as being 10°C above local air temperature used by Reed (1983). They are chemically similar to Crater Lake water, but isotopic data show that they are not leakage from Crater Lake (Thompson and others, 1990). Their anomalous amounts of chloride and sulfate indicate that they have undergone water/rock interaction beyond that of low-temperature weathering (Nathenson and Thompson, 1990). The range in temperature and spring composition shows that the springs are a series of mixed waters with an unknown hot end-member composition. Nathenson and others (1994) have calculated that they represent a convective heat discharge of 87 MW_t (Table 1).

Collier and others (1991) found pools on the floor of Crater Lake with slightly elevated temperatures compared to lake water (Table 3 and Figure 8). Higher temperatures measured in bacterial mats ranged to 19°C, qualifying as a low-temperature geothermal resource using Reed's (1983) definition. The total convective heat discharge into Crater Lake was measured using several techniques and was found to be 15-30 MW_t (Table 1). Dividing this total heat discharge by the 31 km^2 area of the deep part of the lake as represented by the 300-m depth contour yields an average heat flow of 480-970 mW/m^2. Regional heat flow in the high Cascades of Oregon is about 100 mW/m^2 (Blackwell and others, 1990). Thus, this estimate of the average heat flow into the bottom of Crater Lake is approximately 5-10 times the regional value. Heat flow measurements in the sediments of Crater Lake using oceanographic techniques found that 12 out of 62 measurements were higher than 300 mW/m^2, and 7 of those 12 were greater than 550 mW/m^2 (Williams and von Herzen, 1983). Although technically these are "conductive" heat flows because they are calculated as the product of thermal conductivity times the measured temperature gradient, the high values reflect convection of water either through the sediments or localized in a nearby vent. Some of the pattern of high measured heat flow values (Figure 8) is confirmed by the locations of fluid venting reported by Collier and others (1991) and also shown in Figure 8. Collier and others (1991) were unable to make a systematic search of the caldera floor for other locations of fluid venting, but it seems likely, based on the heat flow survey, that there are additional areas where active fluid venting is taking place.

The convective heat discharge into Crater Lake is the third largest in the United States part of the Cascades; only Austin Hot Springs (at 36 MW_t; Mariner and others, 1990) and Lassen Volcanic National Park (120 MW_t; Sorey and Colvard, 1994) are larger. The convective heat discharge from the springs in the vicinity of the Wood River of 87 MW_t is close to the value for Lassen. The implication of the large convective heat discharge apparently from Mount Mazama in the Wood River area is that there must be a high heat loss associated with some remnant of the climactic magma chamber. Accepting a hydrothermal heat-transfer rate of about 102 MW_t from the springs in the vicinity of the Wood River and from the inflow to Crater Lake and assuming that the rate of heat loss has been at least that value for the last 7700 years, the total heat loss is 25×10^{18} joules (Table 1), or 6% of the total heat content of the magma chamber after the climactic eruption 7700 years ago. Smith and Shaw (1975) estimate that the conductive heat transfer over the last 700 years was 17×10^{18} joules, assuming that the magma chamber began conductive heat loss at that time and that it had a surface area of 50 km^2. More recent data indicate that the magma body probably has been cooling for about 7700 years and that the chamber area may be closer to 20 km^2 than 50 km^2. The corresponding calculation would result in somewhat greater total conductive heat transfer of 21×10^{18} joules (Table 1).

Subsurface thermal data

Figure 3 shows temperature data (Blackwell and Steele, 1987; Blackwell, 1994) from the two industry drill holes on the flanks of Mount Mazama (Figure 1) along with a line showing a 50°C/km regional geothermal gradient for the Cascades. Geologic interpretations of drill core also are presented in Figure 3. Hole MZII-1 located near the south boundary of the park shows a variable pattern of temperatures as a function of depth that may partly reflect disturbance from drilling. However, temperatures are notably high at shallow depths. The drill hole is within the Klamath graben, 4 km west of the East Klamath Lake fault zone that controls the locations of springs near the Wood River and may penetrate the warm aquifer feeding these springs. Three km west of the drill hole, late Pleistocene basaltic andesite dives beneath intervening pyroclastic-flow deposits of the climactic eruption and may be projected toward the hole. The massive basaltic andesite and basalt sill(?) encountered by the drill hole at 342-756 m may restrict water flow to zones above and below. Flow is likely in the porous top of the lava flow below the sill that is part of a >111-m-thick section of basalt or basaltic andesite lava flows.

Hole MZI-11A is located just east of the park boundary (Figure 1). The first temperature log (Blackwell and Steele, 1987) was taken when the hole was 413 m deep (Priest and others, 1987) with data to 405 m. When the second temperature log was taken, the water level in the open pipe in the drill hole was at 372 m (La Fleur, 1990). The water level corresponds to the region of high gradient in lava flows and breccias of the hornblende-bearing andesite/dacite volcano near the bottom of the first log. Data taken above the water level in the second log have not been included on Figure 3. Neither temperature log is likely to have measured equilibrium temperatures; the second log was taken 46 days after drilling ceased on August 8, 1989. The maximum temperature measured is 129.6°C at a depth of 1067 m, within a 100-m-thick section of andesite lava flows containing a sill. The maximum temperature occurs just above the base of a 9-m-thick lava flow, 8 m above the top of the 19-m-thick sill. Sedimentary horizons within this part of the lava section have apparent dips of 16-34°. The slight reversal in temperature may indicate that a zone of horizontal flow of hot water was intersected by the drill hole within the andesite lava flow section. Below 1113 m the drill hole penetrated intermediate and silicic pyroclastic rocks, mostly pyroclastic flows but including reworked material with an apparent dip of 22° at 1205 m, possibly correlative with Tertiary Western Cascade rocks. Dips may increase downward because a pyroclastic-flow base has an apparent dip of 36° at 1423 m, virtually at the bottom of the hole. Fracture fillings common in the lava and breccia section above 1113 m are scarce in the pyroclastic flows below that depth.

Alteration is ubiquitous in core from hole MZI-11A, beginning in the ≥400 ka pre-Mazama rhyodacite lava. Overlying, fresh andesite of Scott Creek is late Pleistocene in age. Hull and Waibel (1989) reported U-Th disequilibrium data that constrain the age of authigenic calcite in samples from 262 to 389 m depth, all within the hornblende dacite lava flows and breccias beneath pre-Mazama rhyodacite (Figure 3). Results for most samples imply precipitation ages of >350 ka. None yielded an apparent age <120-160 ka. The hydrothermal system which deposited the calcite may have been related to early Mount Mazama, including Mount Scott, which was active in the ~350-400 ka interval (Bacon and Lanphere, 1990).

Figure 10 is a cross section from the southwest quadrant of the caldera, through drill hole MZI-11A, ending east of the pre-Mazama rhyodacite field (Figure 1, A-A'). The area of bacterial mats on the lake floor is shown. Anderson Spring is from a perched water table, defined by the base of unconsolidated pyroclastic-flow deposits of the climactic eruption (lithic breccia of Druitt and Bacon, 1986) like many other non-thermal springs on Mount Mazama, well above the water table indicated by the level of Crater Lake and the drill hole. The water level in MZI-11A is 407 m below the level of Crater Lake. Sammel and Benson (1987) modeled the hydrologic system of Mount Mazama, with one of their cross sections being just slightly north of section A-A' shown in Figure 1. Their model was able to reproduce the water level measured in this drill hole using leakage from the lake and a regional water table defined by Klamath Marsh to the east. The flow direction near the water table at the location of the drill hole is generally horizontal with a slight downward component. The high temperatures found near the water table in the drill hole are not well explained by their model. This may indicate that, in this sector, there is actually very little leakage from the lake and the water table is set by a balance of recharge and regional discharge. Recharge in the high-elevation area near the lake may actually be limited, because the downward flowing water is forced outward in perched aquifers such as that feeding Anderson Spring.

Water geochemistry

Chemical data for fluid samples are given in Table 3 for the deep part of the lake, Llao's Bath and a Palisade Point pool from the floor of the lake, and the source of Crooked Creek as the most concentrated sample of the springs in the vicinity of the Wood River. These data can be used to address the relation between pool chemistry and lake chemistry and the relation between the various concentrated samples. Fluid-chemistry samples from Llao's Bath and the Palisade Point pool (Table 3) show enrichment in those elements necessary to explain the composition of Crater Lake compared to the available water supply from precipitation and runoff from the caldera walls (Collier and others, 1991). Table 4 presents the major-ion chemistry as equivalent percents and ion mass ratios for selected constituents. The equivalent percentages shown in Table 4 for magnesium and chloride, for example, indicate that the waters from the pools are different in relative concentrations from each other and from that in Crater Lake (see also Figure 11). This difference in relative concentrations can be more easily assessed from the mass ratios in the last two columns of the table. The ratio Na/Cl is 1.0 in the lake, but it is 1.8 and 2.9 in the pools. Assuming that the major determinant of lake chemistry is the concentrated inflows, there are two possibilities to explain this difference. One interpretation is that the major fluid source feeding the lake has not yet been found. A second is that the hydrothermal system at Crater Lake is evolving, and that the chemistry of the warm water has recently (but more than 50 years ago, Nathenson [1990b]) changed. An indication that this might be the case is the discovery of apparently inactive silica spires near Skell Head in the north basin southeast of the Palisade Point pools (Figure 8). The precipitation of silica indicates a higher temperature at these locations than any yet measured on the lake floor. The sample from the source of Crooked Creek is most similar to Crater Lake water (Figure 11), although it has a notably lower lithium concentration (Table 3). The difference in silica concentrations is partly explained by diatoms consuming silica in Crater Lake water (Nathenson, 1990b).

Stable isotopes

The stable isotopic compositions of water for samples from Llao's Bath and the Palisade Point pool show that the source of the water is circulating lake water and that the water has probably not undergone high-temperature (>200°C) reaction with rock (Collier and others, 1991). The water samples from Llao's Bath and the Palisade Point pool have essentially the same hydrogen and oxygen isotopic compositions as lake water. Deuterium values in spring samples in the vicinity of Crater Lake are quite different from lake water, because the hydrogen and oxygen isotopic compositions of precipitation in the lake are modified by evaporation. If the water feeding the pools had a deuterium content similar to that of the springs before mixing with lake water, the pool samples would have to mix with 10 to 20 parts of lake water in order to end up with a deuterium content that is indistinguishable from lake water. The carbon-14 content of the sample from Llao's Bath shows that it can be no more than 50 % unmodified lake water (Collier and others, 1991). The dissolved oxygen content of the sample for the Palisade Point pool is very low, indicating very little mixing with well-oxygenated lake water (Collier and others, 1991). Thus, the deuterium contents of the pools are only slightly modified from that for the fluid that feeds the pools, and the source of the fluid in the pools is lake water that has circulated to depth to be heated and react with rock. Like that of hydrogen, the oxygen isotopic composition of lake water also is modified by evaporation, and it can undergo additional change if water reacts with rock at high temperature. Collier and others (1991) have calculated the change in oxygen isotopic composition of water for various ratios of water to rock as a function of temperature. Unless the water to rock ratio is very high, the similarity of the oxygen isotopic composition of the pool samples and lake water indicates that equilibration temperatures are less than 200°C.

Chemical geothermometry

Chemical geothermometer temperatures calculated from major-element concentrations for the pool samples suggest that inflow temperatures are higher than measured temperatures (Table 3). The calculation of geothermometer temperatures for the composition of lake water is not strictly appropriate, because the lake water is clearly a mixture of a more saline water with water from precipitation and springs on the caldera walls. The pools provide more appropriate samples for geothermometer calculations, but their high magnesium concentrations compared to calcium and potassium concentrations indicates caution in using geothermometer temperatures. In most thermal waters, magnesium concentrations are very low, because magnesium preferentially stays in the solid phase when water reacts with volcanic rock at elevated temperatures. Accordingly, in some waters, high magnesium concentrations indicate that the water is equilibrated at low temperature. However, in other cases, high magnesium concentrations are caused by mixing a higher-temperature water with a cold water and subsequent reaction at the mixed temperature. Geothermometer temperatures (chalcedony, Mg-Li, K-Mg) for Llao's Bath range from 50° to 90°C and for Palisade Point pool from 35° to 70°C. Based on the high magnesium concentration, the Mg-corrected Na-K-Ca geothermometer relations of Fournier and Potter (1979) would indicate that the water has equilibrated at the spring temperature (for example the 19°C temperature measured in one mat). Collier and others (1991) report Na-Li geothermometer temperatures of 165°C for Llao's Bath and 110°C for Palisade Point pool, but these high temperatures are not corroborated by other geothermometers. Na-K temperatures are 245°C for Llao's Bath and 151°C for the Palisades Point pool, but the Na-K geothermometer is not reliable for low-temperature waters.

Helium isotopes

Collier and others (1991) have made an extensive study of helium isotope systematics for Crater Lake and pool water samples. They found that the warm water flowing into the lake has $^3He/^4He$ ratios characteristic of mantle sources. The usual interpretation of such a mantle signature in a volcanic area is that the excess ^3He was exsolved from magma, along with other volatiles, during ascent and crystallization. Helium derived from the degassing magma is then incorporated in and transported further by the water. This can be used to argue that there may be higher fluid temperatures than any geothermometers have indicated but also is consistent with long-term degassing of subsurface magma whether or not a high-temperature hydrothermal system is present.

Comparison with Mount Hood

An interesting comparison can be made to Swim Warm Springs on the flanks of Mt. Hood, Oregon. The measured spring temperatures there range to 26°C, and the geothermometer temperatures (including sulfate oxygen isotopic equilibrium) range from 30° to 110°C (Table 3), also with high magnesium contents (Wollenberg and others, 1979; Mariner and others, 1990). The chemistry of Swim Warm Springs (Figure 11) is interpreted by Wollenberg and others (1979) to result from a higher temperature water (≈110°C to 150°-200°C) from near the central vent of the Mount Hood volcano flowing in the subsurface, mixing with cold water, and re-equilibrating some of its constituents to the mixing temperature. A similar model, but with the higher temperature water originating in or beneath caldera fill, could explain the chemistry of waters sampled in the two pools in Crater Lake.

Geothermal resources

The igneous history of Mount Mazama, Crater Lake caldera, and their surroundings indicate that substantial mid- to upper-crustal magmatic heat sources have been present at several times in the Quaternary. The remains of the most recent shallow magma chamber and its wallrocks must still contain a large quantity of heat ($\geq 375 \times 10^{18}$ joule; Table 1) that could support active geothermal systems. The case for geothermal resources is strengthened by the evidence for tectonic extension, which should facilitate circulation of fluids in fault zones and related fracture systems.

Evaluation of active hydrothermal systems is based on the temperature and chemistry of spring and lake waters and on data from two exploration wells. The similar but not quite identical chemistry of the source of Crooked Creek (as representative of the Wood River group of springs) compared to Crater Lake water indicates that the water has undergone a similar water/rock interaction, but it is not part of the same hydrothermal system. The differing chemistry of Llao's Bath and the Palisade Point pool from each other and from the major inflow of warm water to Crater Lake may indicate that processes in the near-surface of the lake floor are important in determining the chemistry of warm water or that there are some very local circulation systems within the lake floor. The known chemistry does not indicate reservoir temperatures higher than about 90°C. Although one can argue that the outflow zone of the springs in the Wood River Valley may actually represent a separate system, geothermometer temperatures for the outflow and springs within the lake are reasonably similar, and so little is known about the characteristics of the hot end-member for either system that lumping them as a single system is reasonable. This geothermal system is likely to be entirely within the National Park and could be called the *Crater Lake hydrothermal system.*

The system within the caldera and extending with the outflow zone to the south may reasonably be assumed to have a minimum temperature of 40°C, a maximum of 100°C, and a most likely of 50°C. Because of the large convective heat discharge, wide-scale distribution of vents, and high heat flow within the caldera, areas should be set at minimum = 10 km^2 (ring fracture fault zone; Nelson and others, 1988), most likely = 20 km^2 (minimum area of magma chamber), and maximum = 40 km^2 (area of most of caldera). For perspective, the area of the lake is 53 km^2, and the area of the 300-m depth contour is 31 km^2. For thickness, we use the default values of Brook and others (1979) of 1, 1.5, and 2.5 km. Applying the methodology of Brook and others (1979), the stored thermal energy is $5.1 \pm 2.2 \times 10^{18}$ joules.

The drill hole MZI-11A intersected a hydrothermal system that does not appear to be contiguous with the Crater Lake system. A reasonable interpretation of the 130°C measured in drill hole MZI-11A, which is not readily explainable from the geothermometer data obtained from any spring sample, is that it is related to a different circulation system from that feeding warm springs in the lake. Based on these notions of separateness, it is proposed that the hydrothermal system associated with the drill hole be given most-likely and minimum temperatures of 130°C and a maximum temperature of 150°C. There are no data to support any estimate of area, and it is proposed that the system be assigned default minimum and most likely areas of 1 and 2 km^2. One can argue that the drill hole has sampled an outflow zone on the edge of a hydrothermal system. The heat source could be from relatively young intrusive rocks related to 70 ka dacites near the caldera rim, and the area of the system could be defined as a circle between the caldera rim and the drill hole or 28 km^2 maximum area. With the default areas, the system can be assumed to lie half inside and half outside of the National Park. For the speculative maximum area, the system would lie almost entirely within the National Park. For thickness, we use the default values of Brook and others (1979) of 1, 1.5, and 2.5 km. Based on the drill hole being in the Mazama unit of the Winema National Forest, the hydrothermal system could be called the *Mazama hydrothermal system.* Applying the methodology of Brook and others (1979), the stored thermal energy is $5.7 \pm 3.6 \times 10^{18}$ joules.

Brook and others (1979) did not estimate stored thermal energy for the hydrothermal systems in the Crater Lake area because there were almost no data with which to characterize them. Bloomquist and others (1985) use the area within which the Curie isotherm is 5-7 km below sea level for their estimate of the area of the thermal anomaly associated with Crater Lake. They use the regional conductive thermal structure for the Oregon Cascades to define the thermal structure and reservoir thickness. Mean temperature is 185°C, and mean reservoir area is 3150 km^2. Their calculated stored thermal energy above 5°C is $1630 \pm 760 \times 10^{18}$ joules (above 15°C, $1540 \pm 720 \times 10^{18}$ joules), over two orders of magnitude larger than the values calculated in this study. The major difference is the estimate of subsurface area. The use of the area of anomalous depth to Curie isotherm to define a reservoir area is speculative and leads to a very large value (3150 km^2; the area of the Crater Lake magma chamber as proposed in this study is only 20 km^2). The area of monogenetic volcanoes in Figure 1 is quite large, but these are unlikely to represent much of a thermal anomaly in the upper 3 km. Although there is still considerable uncertainty in the temperature and area of the thermal anomaly at Crater Lake, it does not seem likely that it is anywhere near as large or as hot as proposed by Bloomquist and others (1985).

Black (1994) also used a conductive thermal regime to estimate resources in the Cascades by township-sized blocks. He did not assess the thermal energy in hydrothermal systems but defers to Brook and others (1979) for those values. Under the township that includes MZI-11A, Black (1994) estimates a temperature of 150°C at 2.25 km and 190°C at 3 km, based on a thermal gradient of 53.3°C/km and a heat flow of 112 mW/m^2. Although the temperature values are reasonable, they are a bit optimistic based on the temperature log shown in Figure 3. However, this thermal regime is also proposed to underlie a strip 2 or 3 sections wide stretching north and south through Crater Lake, including the area of MZII-1. The data for MZI-11A clearly indicate the existence of a hydrothermal system that invalidates the use of a regional conductive thermal model to assess geothermal resources between 0 and 3 km. The data for MZII-1 probably also indicate a hydrothermal system. Whether the regional thermal model is valid away from the immediate vicinity of Mount Mazama is unclear based on the available data.

Acknowledgments

The Superintendent of Crater Lake National Park granted us permission to conduct field work in the park and park staff provided logistical support for lake floor studies. Robert Collier, Jack Dymond, and their associates at Oregon State University shared data on hydrothermal inputs into Crater Lake. Mark Buktenica of Crater Lake National Park, Collier, and Dymond piloted the submersible Deep Rover, operated by Can-Dive Services of Vancouver, B.C., during the dives dedicated to geology. California Energy Company provided access to drill core from the two exploration wells. We thank Al Waibel and Joe La Fleur for their cooperation in drill core studies. Ruth Ludwin kindly re-located the 1982 earthquake epicenter and helped to clarify the record of seismicity for the Crater Lake area. Patrick Muffler and Marianne Guffanti reviewed an early version of the manuscript. Further reviews by Muffler and by Michael Ryan helped us to improve the final document.

References

Bacon, C. R., 1983, Eruptive history of Mount Mazama and Crater Lake caldera, Cascade Range, U.S.A.: Journal of Volcanology and Geothermal Research, v. 18, p. 57-115.

Bacon, C. R., 1990, Calc-alkaline, shoshonitic, and primitive tholeiitic lavas from monogenetic volcanoes near Crater Lake, Oregon: Journal of Petrology, v. 31, p.135-166.

Bacon, C. R., 1992, Partially melted granodiorite and related rocks ejected from Crater Lake caldera, Oregon: Transactions of the Royal Society of Edinburgh: Earth Sciences, v. 83, p. 27-47.

Bacon, C. R., and Druitt, T. H., 1988, Compositional evolution of the zoned calcalkaline magma chamber of Mount Mazama, Crater Lake, Oregon: Contributions to Mineralogy and Petrology, v. 98, p. 224-256.

Bacon, C. R., and Lanphere, M. A., 1990, The geologic setting of Crater Lake, Oregon, *in* Drake, E. T., Larson, G. L., Dymond, J., and Collier, R., eds., Crater Lake, An Ecosystem Study: Pacific Division, American Association for the Advancement of Science, San Francisco, p. 19-27.

Bacon, C. R., Adami, L. H., and Lanphere, M. A., 1989, Direct evidence for the origin of low-^{18}O silicic magmas: quenched samples of a magma chamber's partially-fused granitoid walls, Crater Lake, Oregon: Earth and Planetary Science Letters, v. 96, p. 199-208.

Bacon, C. R., Gunn, S. H., Lanphere, M. A., and Wooden, J. W., 1994, Multiple isotopic components in Quaternary volcanic rocks of the Cascade arc near Crater Lake, Oregon: Journal of Petrology, v. 35, p. 1521-1556.

Bacon, C. R., Mastin, L. G., Scott, K. M., and Nathenson, Manuel, in preparation, Volcano and earthquake hazards in the Crater Lake region, Oregon: U.S. Geological Survey Open-File Report.

Bacon, C. R., Newman, S., and Stolper, E., 1992, Water, CO_2, Cl, and F in melt inclusions in phenocrysts from three

Holocene explosive eruptions, Crater Lake, Oregon: American Mineralogist, v. 77, p. 1021-1030.
Berg, J. W., Jr., and Baker, C. D., 1963, Oregon earthquakes, 1841 through 1958: Bulletin of the Seismological Society of America, v. 53, p. 95-108.
Black, G. L., 1994, Geothermal electrical power generation potential of Newberry Volcano and the Oregon Cascade Range: Oregon Department of Geology and Mineral Industries, Open-File Report O-94-07, p. 1-73.
Blackwell, D. D., 1994, A summary of deep thermal data from the Cascade Range and analysis of the "rain curtain" effect: Oregon Department of Geology and Mineral Industries, Open-File Report O-94-07, p. 75-131.
Blackwell, D. D., and Steele, J. L., 1987, Geothermal data from deep holes in the Oregon Cascade Range: Geothermal Resources Council Transactions, v. 11, p. 317-322.
Blackwell, D. D., Steele, J. L., Frohme, M. K., Murphey, C. F., Priest, G. R., and Black, G. L., 1990, Heat flow in the Oregon Cascade Range and its correlation with regional gravity, Curie point depths, and geology: Journal of Geophysical Research, v. 95, p. 19,475-19,493.
Blank, H. R., Jr., 1968, Aeromagnetic and gravity surveys of the Crater Lake region, Oregon, *in* Dole, H. M., ed., Andesite Conference Guidebook, Oregon Department of Geology and Mineral Industries, Bulletin 62, p. 42-52.
Bloomquist, R. G., Black, G. L., Parker, D. S., Sifford, A., Simpson, S. J., and Street, L. V., 1985, Evaluation and ranking of geothermal resources for electrical generation or electrical offset in Idaho, Montana, Oregon and Washington: Washington State Energy Office, WAOENG-85-02a, 504p.
Brook, C. A., Mariner, R. H., Mabey, D. R., Swanson, J. R., Guffanti, Marianne, and Muffler, L. J. P., 1979, Hydrothermal convection systems with reservoir temperatures ≥ 90°C, *in* Muffler, L. J. P., ed., Assessment of geothermal resources of the United States—1978: U.S. Geological Survey Circular 790, p. 18-85.
Clynne, M. A., 1990, Stratigraphic, lithologic, and major element geochemical constraints on magmatic evolution at Lassen volcanic center, California: Journal of Geophysical Research, v. 95, p. 19,651-19,669.
Collier, R. W., Dymond, Jack, and McManus, James, 1991, Studies of Hydrothermal Processes in Crater Lake, OR: College of Oceanography Report #90-7, Oregon State University, 317 p.
Dobrin, M. B., 1952, Introduction to Geophysical Prospecting: McGraw Hill, New York, 435 p.
Druitt, T. H., and Bacon, C. R., 1986, Lithic breccia and ignimbrite erupted during the collapse of Crater Lake caldera, Oregon: Journal of Volcanology and Geothermal Research, v. 29, p. 1-32.
Druitt, T. H., and Bacon, C. R., 1988, Compositional zonation and cumulus processes in the Mount Mazama magma chamber, Crater Lake, Oregon: Transactions of the Royal Society of Edinburgh: Earth Sciences, v. 79, p. 289-297.
Druitt, T. H., and Bacon, C. R., 1989, Petrology of the zoned calcalkaline magma chamber of Mount Mazama, Crater Lake, Oregon: Contributions to Mineralogy and Petrology, v. 101, 245-259.
Fiske, R. S., Hopson, C. A., and Waters, A. C., 1963, Geology of Mount Rainier National Park, Washington: U.S. Geological Survey Professional Paper 444, 93 p.
Fournier, R. O., and Potter, R. W., II, 1979, Magnesium correction to the Na-K-Ca chemical geothermometer: Geochimica et Cosmochimica Acta, v. 43, p. 1543-1550.
Goter, S. K., 1994, Earthquakes in Washington and Oregon, 1872-1993: U.S. Geological Survey Open-File Report 94-226A, 1 sheet, scale 1:1,000,000.
Hart, W. K., Aronson, J. L., and Mertzman, S. A., 1984, Areal distribution and age of low-K, high-alumina olivine tholeiite magmatism in the northwestern Great

Basin: Geological Society of America Bulletin, v. 95, p. 186-195.

Hawkins, F. F., Foley, L. L., and LaForge, R. C., 1989, Seismotectonic study for Fish Lake and Fourmile Lake dams, Rogue River Basin Project, Oregon: U.S. Bureau of Reclamation, Denver, Colorado, Seismotectonic Report 89-3, 26 p.

Hildreth, Wes, and Lanphere, M. A., 1994, Potassium-argon geochronology of a basalt-andesite-dacite arc system: The Mount Adams volcanic field, Cascade Range of southern Washington: Geological Society of America Bulletin, v. 106, p. 1413-1429.

Hull, C. D., and Waibel, A. F., 1989, U-Th disequilibrium dating of authigenic calcites in the Mazama (MZI-11A) geothermal well, Oregon: Geothermal Resources Council Transactions, v. 13, p. 157-163.

Jacobson, R. S., 1986, Map of Oregon seismicity, 1841-1986: Oregon Department of Geology and Mineral Industries, Geological Map Series GMS-49, 1 sheet, scale 1:1,000,000.

Kollmann, A., and Zollweg, J., 1984, Oregon seismicity - August 1980 to October 1982: U.S. Geological Survey Open-File Report 84-832, 29 p.

La Fleur, Joe, 1990, Letter to Jim Larson, National Park Service: California Energy Co., Santa Rosa, California, 5 p.

Lange, R. L., and Carmichael, I. S. E., 1990, Thermodynamic properties of silicate liquids with emphasis on density, thermal expansion and compressibility: *in* Nicholls, J., and Russell, J.K., eds., Modern Methods of Igneous Petrology: Understanding Magmatic Processes, Mineralogical Society of America Reviews in Mineralogy, v. 24, p. 25-64.

MacLeod, N. S., and Sherrod, D. R., 1992, Reconnaissance geologic map of the west half of the Crescent 1° by 2° quadrangle, central Oregon: U.S. Geological Survey Miscellaneous Investigations Series Map I-2215, scale 1:250,000.

Mariner, R. H., Presser, T. S., Evans, W. C., and Pringle, M. K. W., 1990, Discharge rates of fluid and heat by thermal springs of the Cascade Range, Washington, Oregon, and northern California: Journal of Geophysical Research, v. 95, p. 19,517-19,531.

Nakada, Setsua, Bacon, C. R., and Gartner, A. E., 1994, Origin of phenocrysts and compositional diversity in pre-Mazama rhyodacite lavas, Crater Lake, Oregon: Journal of Petrology, v. 35, p. 127-162.

Nathenson, Manuel, 1990a, Temperatures of springs in the vicinity of Crater Lake, Oregon, in relation to air and ground temperatures: U.S. Geological Survey Open-File Report 90-671, 19 p.

Nathenson, Manuel, 1990b, Chemical balance for major elements in water in Crater Lake, Oregon, *in* Drake, E. T., Larson, G. L., Dymond, J., and Collier, R., eds., Crater Lake, An Ecosystem Study: Pacific Division, American Association for the Advancement of Science, San Francisco, p. 103-114.

Nathenson, Manuel, and Thompson, J. M., 1990 , Chemistry of Crater Lake, Oregon, and nearby springs in relation to weathering, *in* Drake, E. T., Larson, G. L., Dymond, J., and Collier, R., eds., Crater Lake, An Ecosystem Study: Pacific Division, American Association for the Advancement of Science, San Francisco, p. 115-126.

Nathenson, Manuel, Mariner, R. H., and Thompson, J. M., 1994, Convective heat discharge of Wood River group of springs in the vicinity of Crater Lake, Oregon: Geothermal Resources Council, Transactions, v. 18, p. 229-236.

Nelson, C. H, Carlson, P. R., and Bacon, C. R., 1988, The Mount Mazama climactic eruption (~6900 yr B.P.) and resulting convulsive sedimentation on the Crater Lake caldera floor, continent, and ocean basin: Geological Society of America Special Paper 229, p. 37-57.

Nelson, C. H., Bacon, C. R., Robinson, S. W., Adam, D. P., Bradbury, J. P., Barber, J. H., Jr., Schwartz, Deborah, and Vagenas, Ginger, 1994, The volcanic, sedimentologic, and paleolimnologic history of the Crater Lake caldera floor, Oregon: Evidence for small caldera evolution: Geological

Society of America Bulletin, v. 106, p. 684-704.
Priest, G. R., Woller, N. M., Blackwell, D. D., and Gannett, M. W, 1987, Geothermal exploration in Oregon, 1986: Oregon Geology, v. 49, no. 6, p. 67-73.
Qamar, Anthony, and Meagher, K. L., 1993, Precisely locating the Klamath Falls, Oregon, earthquakes: Earthquakes & Volcanoes, v. 24, n. 3, p. 129-139.
Reed, M. J., 1983, Introduction, *in* Reed, M. J., ed., Assessment of low-temperature geothermal resources of the United States — 1982: U.S. Geological Survey Circular 892, p. 1-8.
Robie, R. A., Hemingway, B. S., and Fisher, J. R., 1978, Thermodynamic properties of minerals and related substances at 298.15 K and 1 bar (10^5 Pascals) pressure and at higher temperatures: U. S. Geological Survey Bulletin 1452, 456 p.
Sammel, E. A., and Benson, Sally, 1987, An analysis of the hydrologic effects of proposed test drilling in the Winema National Forest near Crater Lake, Oregon: Geothermal Resources Council Transactions, v. 11, p. 293-303.
Sherrod, D. R., 1991, Geologic map of a part of the Cascade Range between latitudes 43°-44°, central Oregon. U.S. Geological Survey Miscellaneous Investigations Series Map I-1891; scale 1:125,000.
Sherrod, D. R., 1993, Historic and prehistoric earthquakes near Klamath Falls, Oregon: Earthquakes & Volcanoes, v. 24, n. 3, p. 106-120.
Sherrod, D. R., and Pickthorn, L. B. G., 1992, Geologic map of the west half of the Klamath Falls 1° x 2° quadrangle, south-central Oregon: U.S. Geological Survey Miscellaneous Investigations Map I-2182, scale 1:250,000.
Smith, J. G., 1988, Geologic map of the Pelican Butte quadrangle, Klamath County, Oregon: U.S. Geological Survey Geologic Quadrangle Map GQ-1653, scale 1:62,500.
Smith, J. G., Page, N. J., Johnson, M. G., Moring, B. C., and Gray, F., 1982, Preliminary geologic map of the Medford 1°x2° quadrangle, Oregon and California. U.S. Geological Survey Open-file Report 82-955, scale 1:250,000.
Smith, R. L., and Shaw, H. R., 1975, Igneous-related geothermal systems, *in* White, D. E., and Williams, D. L., eds., Assessment of Geothermal Resources of the United States—1975, U.S. Geological Survey Circular 726, p. 58-83.
Sorey, M. L., and Colvard, E. M., 1994, Measurements of heat and mass flow from thermal areas in Lassen Volcanic National Park, California, 1984-93: U.S. Geological Survey Water Resources Investigations Report 94-4180-A, 35 p.
Stebbins, J. F., Carmichael, I. S. E., and Moret, L. K., 1984, Heat capacities and entropies of silicate liquids and glasses: Contributions to Mineralogy and Petrology, v. 86, p. 131-148.
Thompson, J. M., Nathenson, Manuel, and White, L. D., 1990, Chemical and isotopic compositions of waters from Crater Lake, Oregon, and nearby vicinity, *in* Drake, E. T., Larson, G. L., Dymond, J., and Collier, R., eds., Crater Lake, An Ecosystem Study: Pacific Division, American Association for the Advancement of Science, San Francisco, p. 91-102.
Townley, S. D., and Allen, M. W., 1939, Descriptive catalog of earthquakes of the Pacific Coast of the United States 1769 to 1928: Bulletin of the Seismological Society of America, v. 29, p. 1-297.
University of Washington, 1993, Seismicity of Washington and western Oregon, July 1 through September 30, 1993: University of Washington, Geophysics Program, Quarterly Network Report 93-C, 29 p.
Weaver, C. S., 1989, Seismicity of the Cascade Range and adjacent areas, *in* Muffler, L. J. P., Weaver, C. S., and Blackwell, D. D., eds., Geological, Geophysical, and Tectonic Setting of the Cascade Range, U.S. Geological Survey Open-File Report 89-178, p. 74-93.
Westhusing, J. K., 1973, Reconnaissance surveys of near-event seismic activity in the volcanoes of the Cascade Range,

Oregon: Bulletin of Volcanology, v. 37, p. 258-286.

Williams, D. L., and Finn, Carol, 1985, Analysis of gravity data in volcanic terrain and gravity anomalies and subvolcanic intrusions in the Cascade Range, U.S.A., and at other selected volcanoes, *in* Hinze, W. J., ed., The Utility of Regional Gravity and Magnetic Anomaly Maps, Society of Exploration Geophysicists, p. 361-374.

Williams, D. L., Finn, Carol, Couch, R. W., Danes, Z. F., Pitts, G. S., Phillips, W. M., and Riddihough, R. P., 1988, Residual Bouguer gravity anomaly map of the Cascade Range, California, Oregon, Washington, and British Columbia: U.S. Geological Survey Geophysical Investigations Map GP-973, 2 sheets, scale 1:500,000.

Williams, D. L., and Von Herzen, R. P., 1983, On the terrestrial heat flow and physical limnology of Crater Lake, Oregon: Journal of Geophysical Research, v. 88, p. 1094-1104.

Wollenberg, H. A., Bowen, R. E., Bowman, H. R., and Strisower, Beverly, 1979, Geochemical studies of rocks, water, and gases at Mt. Hood, Oregon: Lawrence Berkeley Laboratory Report LBL-7092, 57 p.

Table 1. Estimates of stored heat and heat loss, Crater Lake system. Conductive heat loss rates calculated from Smith and Shaw (1975) are rates at end of period listed.

Heat (10^{18} joules)	Loss rate (MW_t)	Description
		Current convective heat losses from Crater Lake system
—	87	Convective loss represented by Wood River group of springs
—	15-30	Convective loss through floor of Crater Lake
		Thermal budget for Crater Lake magma chamber
230	240	Heat lost to surroundings during growth of climactic magma chamber over ~30,000 yr; loss rate is average for this period
42	22 (at end)	Conductive loss from 20 km^2 chamber over 30,000 yr. (Smith & Shaw, 1975, p. 62)
400	—	Heat stored in magma chamber after climactic eruption
25	102	Minimum convective heat loss since climactic eruption using current rate for last 7700 years
21	44 (at end)	Conductive loss from 20 km^2 chamber in last 7700 yr. (Smith & Shaw, 1975, p. 62)
630	—	Minimum total heat added to the upper crust by presence of 200 km^3 magma chamber and from crystallization before climactic eruption = 400 + 230
375	—	Minimum total heat currently in the upper crust = 630 - 230 - 25
		Smith & Shaw (1975) estimates for Crater Lake magma chamber
770	—	Current heat in 320 km^3 chamber, last eruption 700 yr. ago
17	363 (at end)	Conductive loss from 50 km^2 chamber in last 700 yr.

Table 2. Seismicity in the vicinity of Crater Lake, Oregon.

Date	Time UTC	Lat. Deg	Long. Deg	Depth km	M	NS/NP	Gap Deg	dmin km	RMS sec	Err km	Qual	Mod.	Comment
20/04/14	11:45	42.92	122.10		4+								3 shocks. Intensity V at Fort Klamath
47/10/11	16:	42.75	122.00		3.7								
47/10/12	19:	42.67	122.08		1+								
47/10/14	03:30	42.67	121.92		1+								
82/06/19	08:23	42.904	122.083	0.02*	1.7	6/6	189	53	0.15	2.2	BD	K3	Felt
93/09/21	12:50	42.575	122.181	0.02*	1.9	4/4	309	53	0.29	3.5	BD	K3	
94/01/26	12:33	42.850	122.295	42.07	2.0	8/12	145	31	0.31	1.5	CC	K3	Low frequency event
94/01/28	07:37	42.533	122.058	4.55	1.3	6/8	190	23	0.12	0.5	AD	K3	
94/05/19	03:22	42.673	122.047	6.28	1.7	5/7	214	37	0.08	1.1	BD	K3	
94/05/19	14:35	42.662	122.054	9.29	1.6	6/8	212	36	0.10	0.6	AD	K3	
94/05/20	20:05	42.524	121.680	0.02*	2.4	10/10	165	30	0.21	0.2	BC	K3	Explosion?
94/05/27	18:56	42.554	121.614	17.82	2.1	6/6	259	35	0.16	6.8	CD	K3	
94/12/29	00:21	42.886	122.120	1.48	2.3	9/13	113	45	0.24	1.1	BC	K3	
94/12/29	00:22	42.904	122.113	1.11	2.6	15/16	110	46	0.18	1.1	BC	K3	Felt
94/12/29	00:40	42.892	122.116	1.87$	2.4	13/14	110	46	0.25	9.9	CC	K3	Felt
95/08/13	14:36	42.657	122.056	9.00$	2.0	9/10	111	36	0.14	2.6	BC	K3	
95/08/13	16:18	42.661	122.047	4.28	2.1	13/16	112	36	0.18	1.7	BC	K3	
95/08/13	16:22	42.666	122.040	0.76$	2.0	9/11	112	36	0.28	46.3	DC	K3	

Time is Coordinated Universal Time (UTC). For Pacific Standard Time, subtract 8 hours. For Pacific Daylight Time, subtract 7 hours.
* Depth fixed to an arbitrary values.
$ Maximum number of iterations exceeded. Location and depth are arbitrary.
M - An estimate of the local Richter magnitude. For events after 1982, M is the coda-length magnitude M_C.
NS - number of seismic stations used to locate the earthquake.
NP - number of P and S phases used to calculate location. NS = 3 and NP = 4 are required for a location.
GAP - The central angle of the largest azimuthal sector containing no stations.
RMS - root mean square residual between observed arrival times minus predicted arrival times at all stations used to locate the earthquake.
Err - greater of the values of the vertical or horizontal error estimates.
Qual - Quality factors indicating general reliability of the solution (A is best; D is worst). First letter is a measure of the hypocenter quality based on the arrival time residuals. Second letter is a measure of the quality based on the spatial distribution of stations around the epicenter.
Mod. - crustal velocity model used for earthquake locations.
Locations for 1920 and 1947 events from Jacobson (1986). Times for 1920 and 1947 events from Townley and Allen (1939), Berg and Baker (1963), and Sherrod (1993). Magnitude of 1947 event from Sherrod (1993), and other magnitudes for 1920 and 1947 from Jacobson (1986)
Data for 1982 event from R. S. Ludwin (written communciation, 1996).
Data for 1993 and subsequent events from Pacific Northwest Seismic Network on-line catalogue. Some events have been relocated from preliminary locations given in Quarterly Network Reports (e.g. University of Washington, 1993). An event on 9/21/93 06:08 northeast of the park boundary is so poorly located that it is not included.

Table 3. Concentrations of dissolved constituents and geothermometer temperatures for samples from the deep part of Crater Lake and for pool samples obtained by the submersible (Collier and others, 1991), source of Crooked Creek (Nathenson and Thompson, 1990), and Swim Warm Springs from Mount Hood (Wollenberg and others, 1979).

			Concentrations (mg/L)									Geothermometers					
	T (°C)	pH	SiO_2	Ca	Mg	Na	K	HCO_3	SO_4	Cl	Li	Chalced.	K-Mg	Mg-Li	Na-K-Ca	R-value	Na-K-Ca-Mg
Crater Lake (deep samples)	3.67	6.95	19.7	7.2	2.9	10.8	1.8	39	9.6	10.3	0.05	31[a]	45	41	45	37	NA
Llao's Bath	4.4	7.6	71.4	37.7	27.2	64.4	8.8	303	66	36.5	0.24	91	54	50	76	51.5	33[b]
Palisade Point pool	5	8.91	45.8	25.7	53.7	118.2	4.85	531	81	40.8	0.21	68	35	41	71	75.9	15[b]
Source of Crooked Creek	11	7.9	36.3	8.0	2.4	15.6	1.9	53	6.2	8.4	<0.01	57[a]	47	--	47	31	NA
Swim Warm Spgs Mount Hood	25.6	7.5	72.3	60	48	136	11.7	218	205	161	0.13	91[c]	54	33	83	54.5	27[b]

NA - not applicable.

[a] Chalcedony temperature is a minimum, because water is a mixture of cold and warm waters. Silica concentration in Crater Lake is lowered by diatom consumption.

[b] Magnesium correction is normally not applied when R>50; geothermometer temperature is usually the same as the spring temperature in that case.

[c] Sulfate oxygen temperature is 110°C.

Table 4. Equivalents as percentage of cations and anions, and mass ratios of dissolved constituents in the deep part of Crater Lake, for pool samples obtained by the submersible, source of Crooked Creek, and Swim Warm Springs from Mount Hood.

	Equivalents (%)							Mass ratios	
	Cations				Anions				
	Ca^{+2}	Mg^{+2}	Na^{+}	K^{+}	HCO_3^-	SO_4^{-2}	Cl^-	Na/Cl	SO_4/Cl
Crater Lake (deep samples)	32	21	42	4.2	57	18	26	1.0	0.93
Llao's Bath	26	31	39	3.1	67	19	14	1.8	1.8
Palisade Point pool	12	40	47	1.1	75	15	10	2.9	2.0
Source of Crooked Creek	30	15	51	3.7	70	11	19	1.9	0.7
Swim Warm Springs, Mount Hood	23	30	45	2.3	29	34	37	0.84	1.3

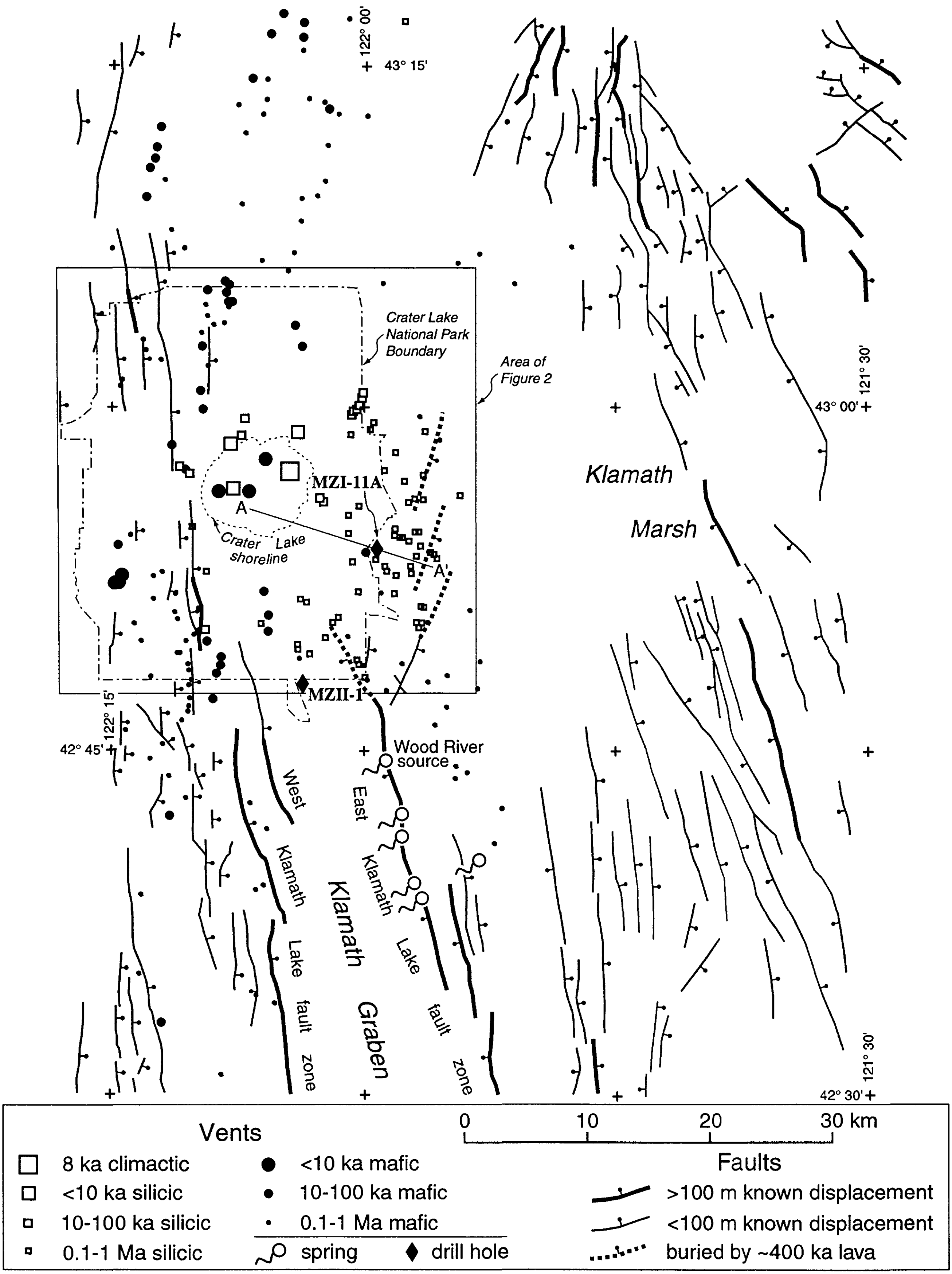

Figure 1. Map of Crater Lake National Park and vicinity showing volcanic vents, faults, locations of drill holes, line of cross section A-A' of Figure 10 (containing MZI-11A), and slightly thermal springs in the vicinity of the Wood River. Vents and faults from MacLeod and Sherrod (1992), Sherrod (1991), Sherrod and Pickthorn (1992), Smith (1988), Smith and others (1982), and C. R. Bacon (unpublished mapping, 1996).

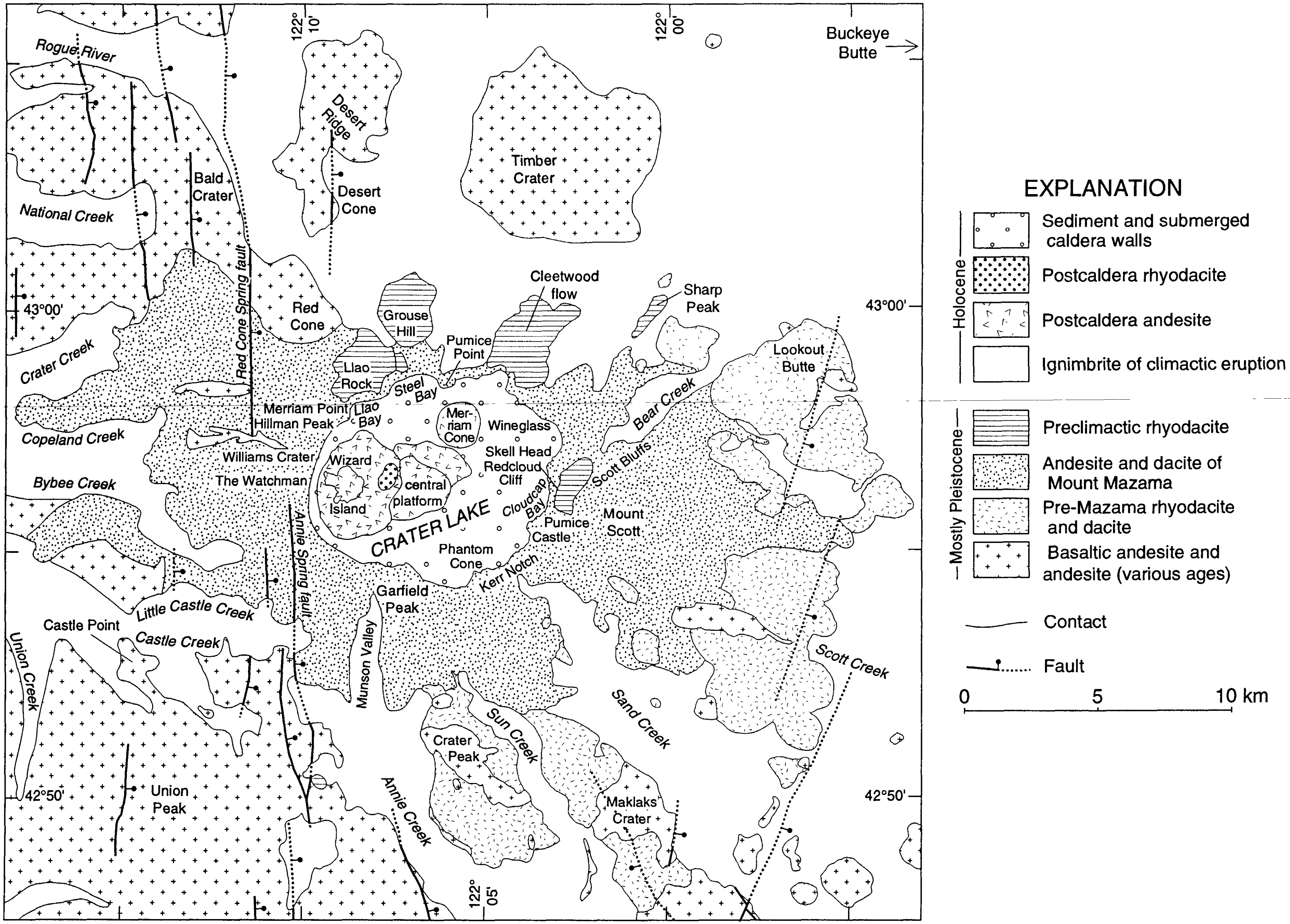

Figure 2. Generalized geologic map of Mount Mazama and vicinity (modified after Bacon and others, 1994).

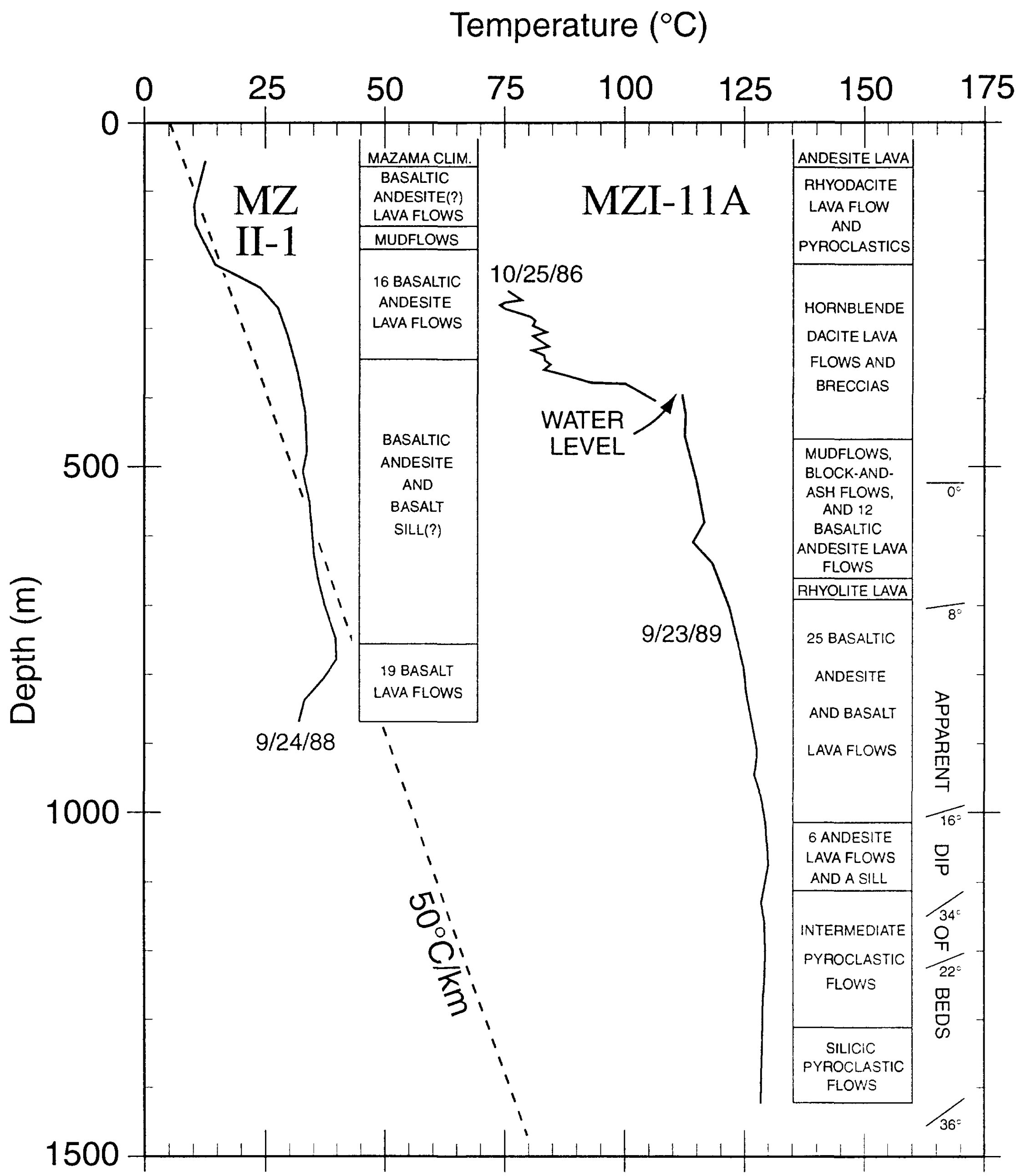

Figure 3. Temperature versus depth data for drill holes on Mount Mazama (Figure 1) from Blackwell and Steele (1987) and Blackwell (1994). Geologic interpretation of drill core by C. R. Bacon (unpublished data, 1996).

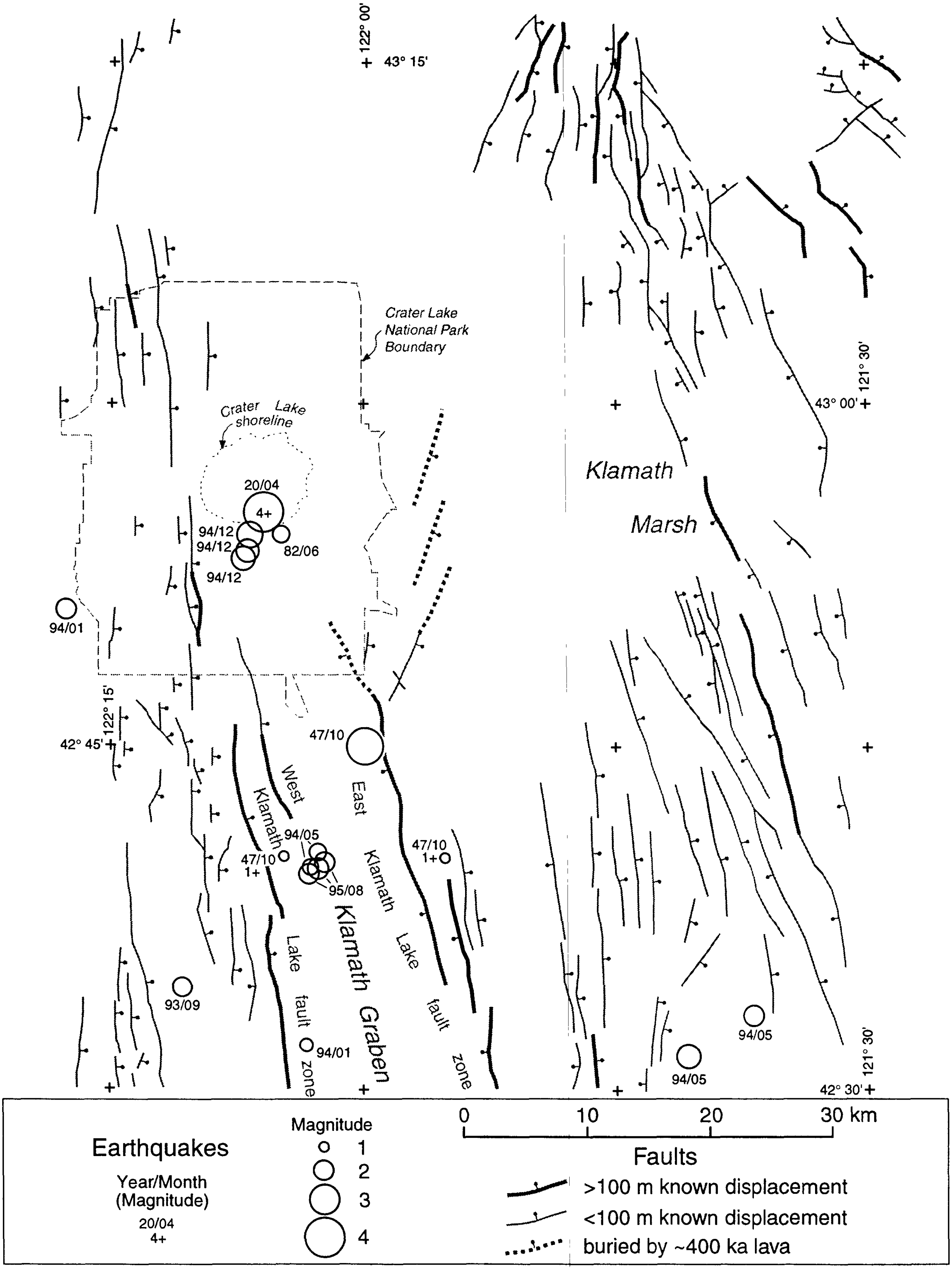

Figure 4. Seismicity of the Crater Lake region (base from Figure 1).

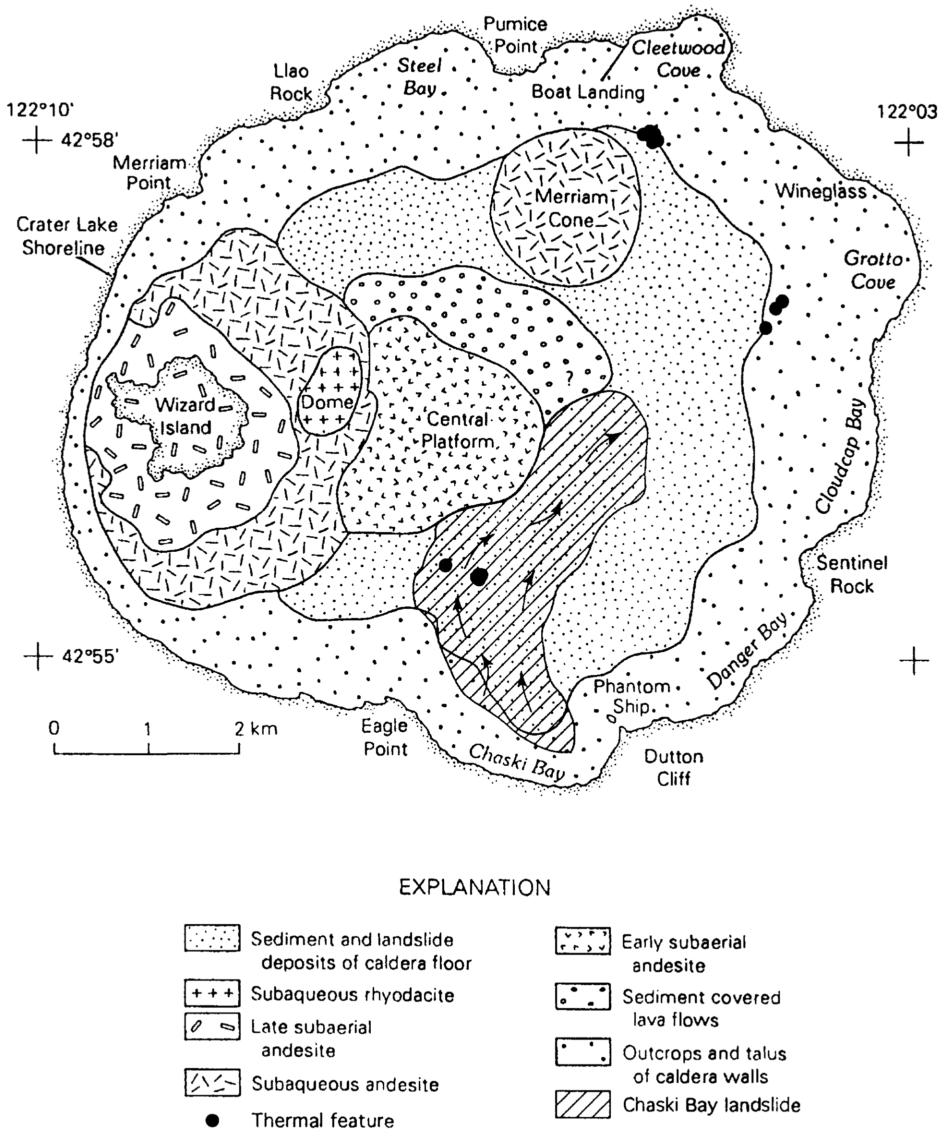

Figure 5. Interpretive geologic map of the floor of Crater Lake caldera (modified after Bacon and Lanphere, 1990, and Nelson and others, 1994).

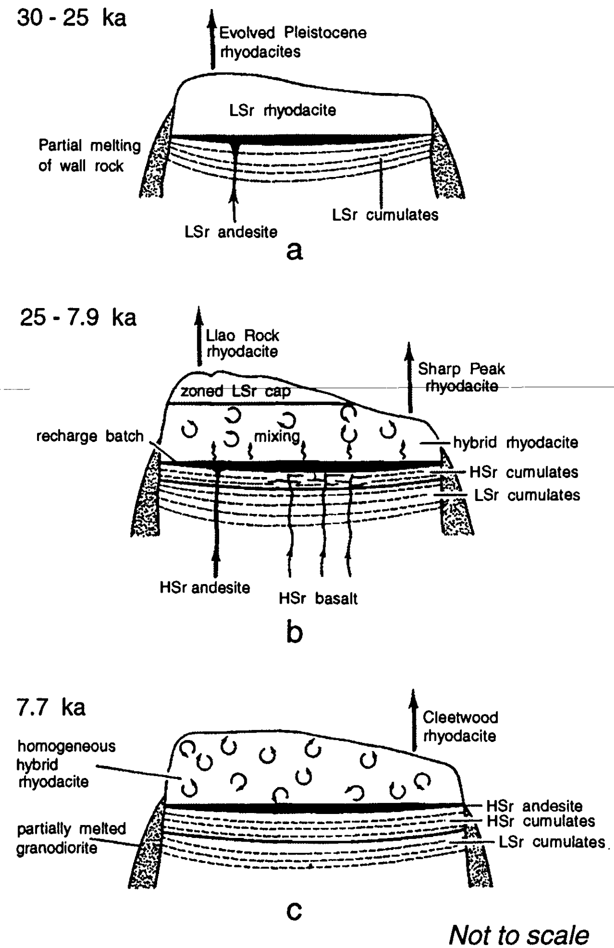

Magma	Magma SiO_2%	Liq. SiO_2%	Vol.% xtls	T °C	Density
Homog. rhyodacite	70	72	10	880	2.2
Zoned HSr magma (incl. mush)	61 53	71 61	28 51	880 950(?)	2.4 2.6
LSr mush	60–51	72–61	50–66	890–>950	2.6–2.8

Figure 7. Summary of the compositional, thermal, and density (crystals plus liquid) zonation in the magma chamber immediately before the climactic eruption (after Druitt and Bacon, 1989).

Figure 6. Model for evolution of the climactic magma chamber by differentiation of andesitic magma ponded between overlying silicic magma and underlying cumulates (modified after Druitt and Bacon, 1989). (a) Early stage represented by eruption of evolved Pleistocene rhyodacites (Grouse Hill, Steel Bay, Redcloud Cliff) derived mainly by fractional crystallization of low-Sr ("LSr") andesitic magma. (b) Development of a zoned cap (Llao Rock) and well-mixed hybrid rhyodacitic magma (Sharp Peak) containing a large component derived by fractional crystallization of high-Sr ("HSr") andesitic magma. (c) Just prior to climactic eruption (Cleetwood).

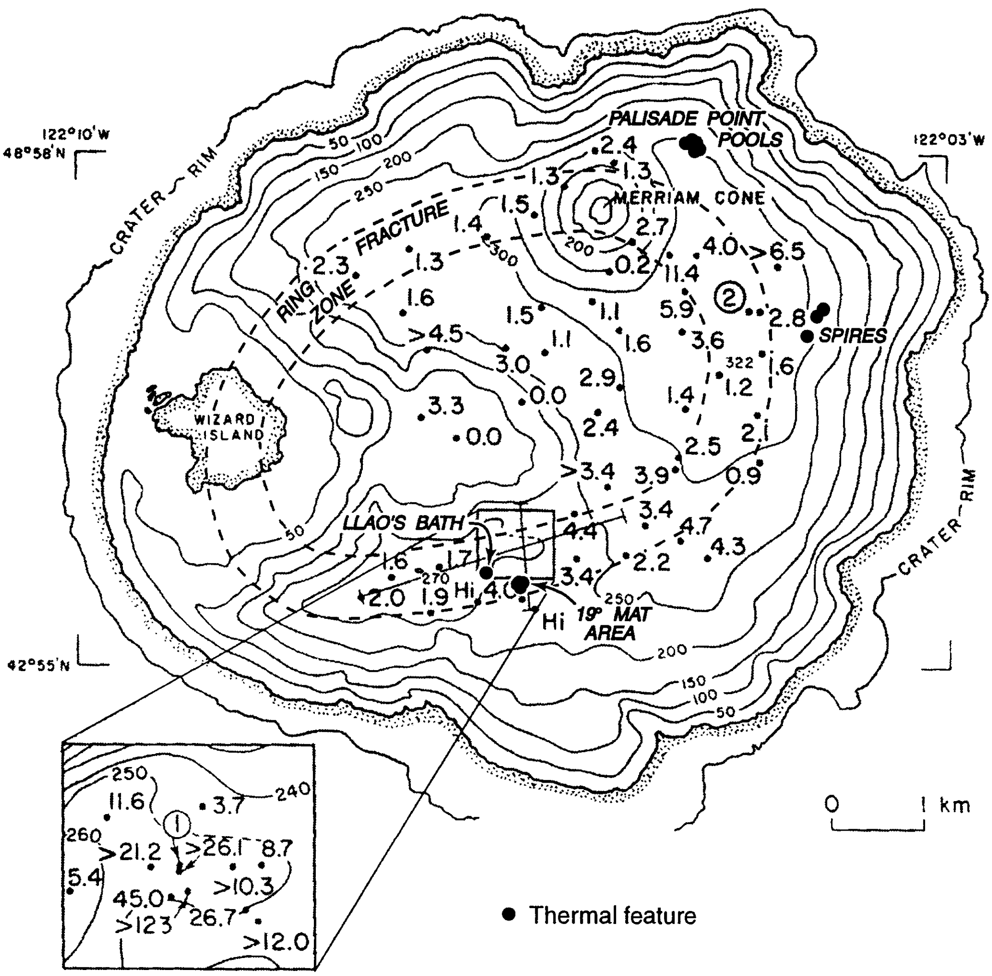

Figure 8. Bathymetric map of Crater Lake (fathoms) showing heat flow (μcal cm^{-2} sec^{-1} = 41.9 mW m^{-2}) values (Williams and Von Herzen, 1983), thermal features (Collier and others, 1991), and hypothesized ring-fracture zone (Nelson and others, 1988).

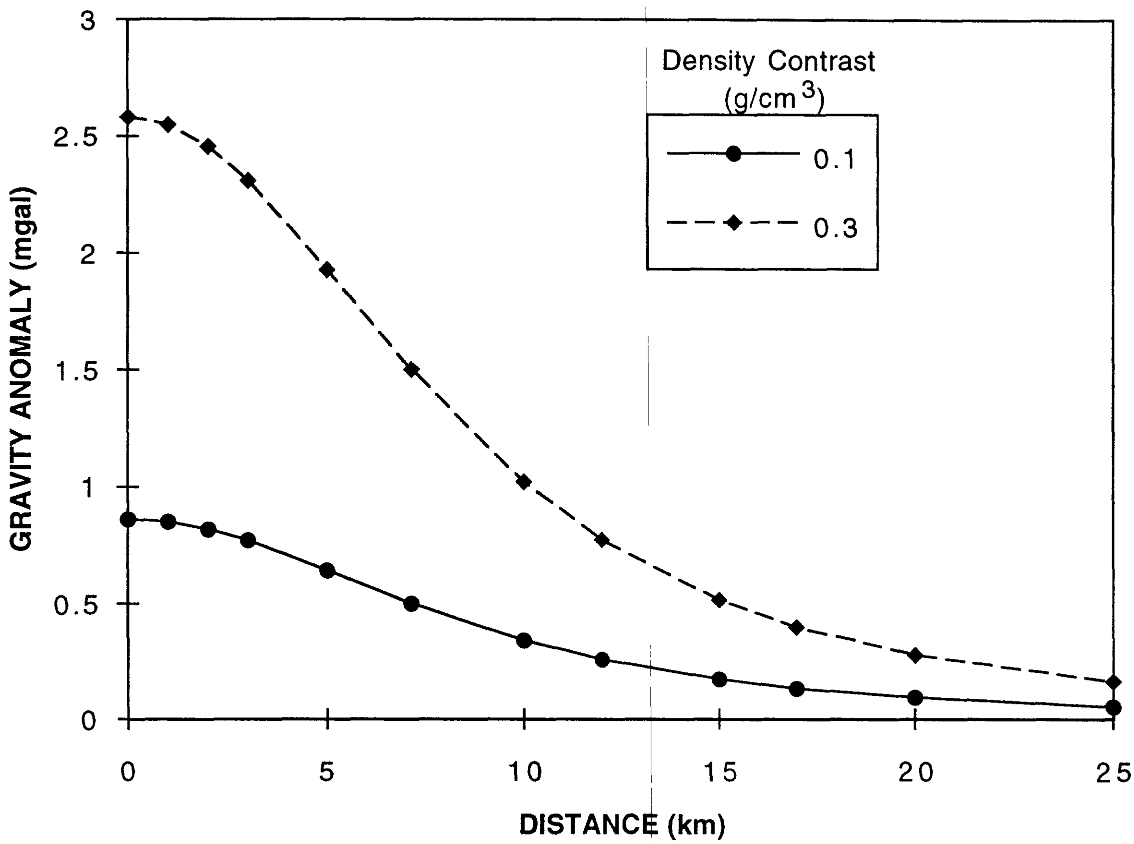

Figure 9. Gravity anomaly for a 6.6-km-diameter sphere with top at 7.5 km depth and two values of density contrast.

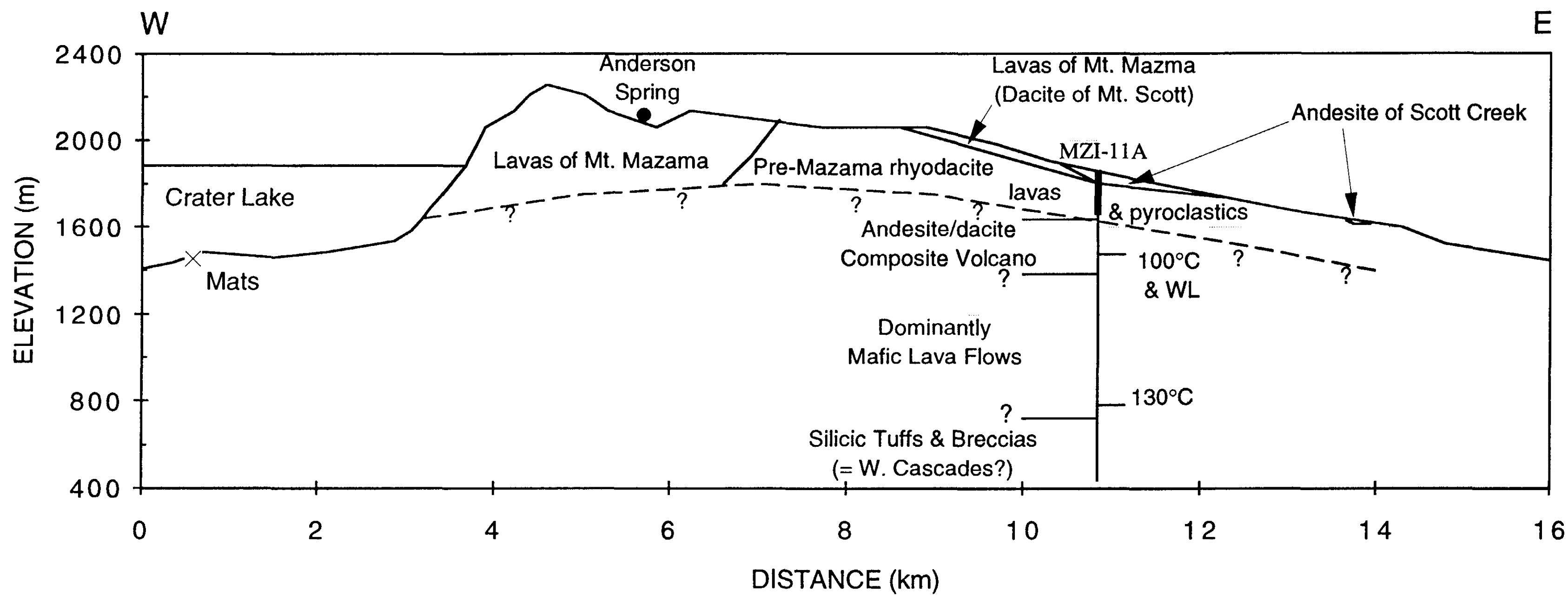

Figure 10. Cross section A-A' from Crater Lake east towards Klamath Marsh. Dashed line indicates possible base of lavas of Mount Mazama and pre-Mazama rhyodacite. See Figure 1 for line of section.

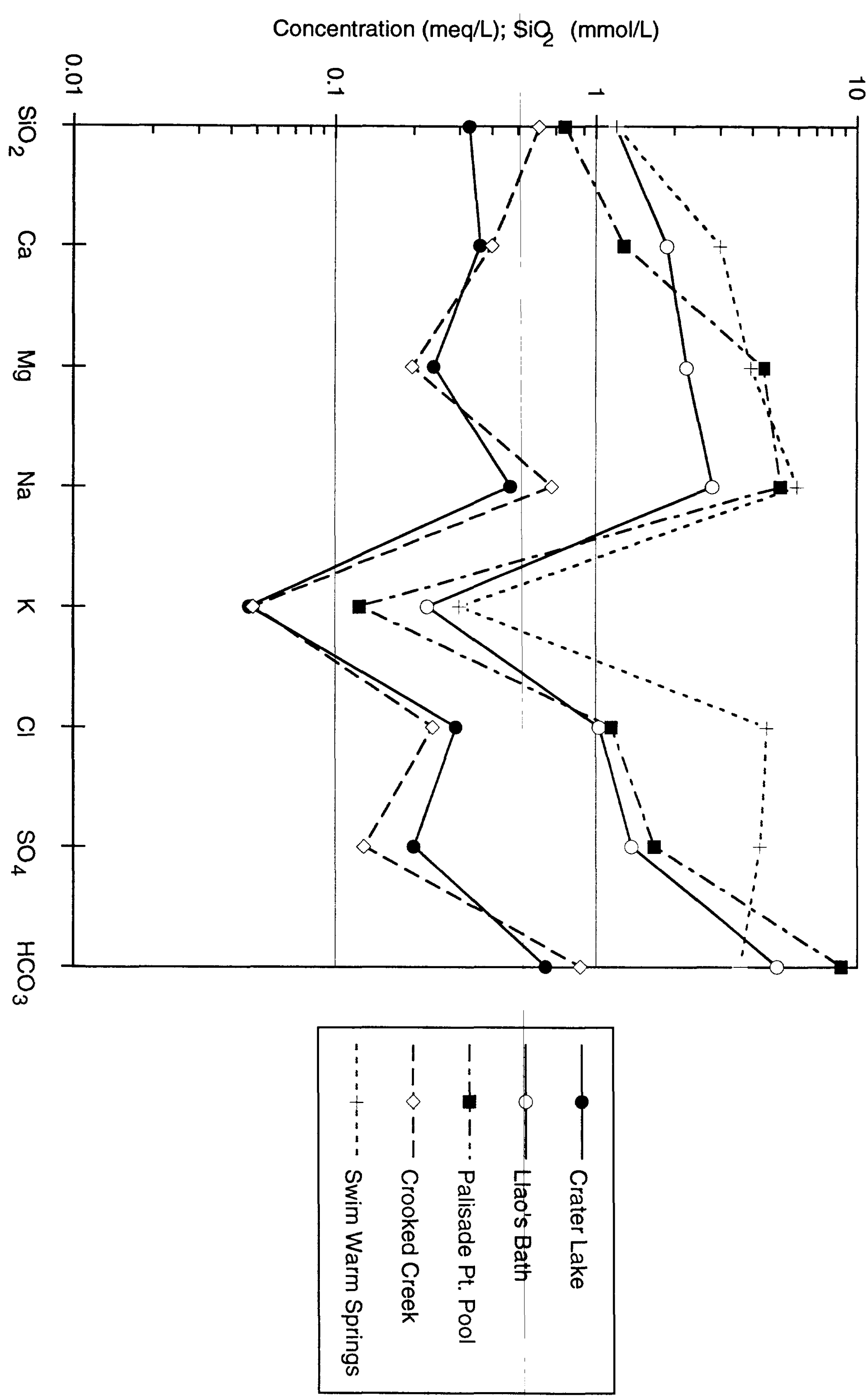

Figure 11. Modified Schoeller diagram for water chemistry of samples given in Table 3.